A SAMPLING TECHNIQUE FOR THE MEASUREMENT OF THE WATER AIR RATIO OF A HIGH SPEED SPRAY LADEN AIR STREAM

R. E. KOSIBA
AND
F. H. E. VOSE

Thesis
K827

DUDLEY KNOX LIBRARY
NAVAL POSTGRADUATE SCHOOL
MONTEREY, CALIFORNIA 93940

Library
U. S. Naval Postgraduate School
Monterey, California

M-51

A SAMPLING TECHNIQUE FOR THE MEASUREMENT OF THE WATER AIR RATIO OF A HIGH SPEED SPRAY LADEN AIR STREAM

by

RICHARD ERWIN KOSIBA, LIEUTENANT JUNIOR GRADE, U.S. NAVY
B.S., U. S. Naval Academy (1947)

and

FREDERIC HARRY EVITT VOSE, LIEUTENANT, U. S. NAVY
B.S., U. S. Naval Academy (1946)

SUBMITTED IN PARTIAL FULFILLMENT

OF THE REQUIREMENTS FOR THE

DEGREE OF NAVAL ENGINEER

at the

MASSACHUSETTS INSTITUTE OF TECHNOLOGY

June 1953

A SAMPLING TECHNIQUE FOR THE MEASUREMENT OF THE WATER AIR RATIO OF A HIGH SPEED SPRAY LADEN AIR STREAM

by

RICHARD E. KOSIBA, LIEUTENANT JUNIOR GRADE, U. S. Navy

and

FREDERIC H. S. WOOD, LIEUTENANT, U. S. NAVY

Submitted to the Department of Naval Architecture and Marine Engineering on May 25, 1943, in partial fulfillment of the requirements for the degree of Naval Engineer.

ABSTRACT

The object of this investigation was to develop a sampling technique for measuring the water-air ratio of a high speed spray laden air stream, including the design of a probe which would withdraw a truly representative sample of the total water (liquid and vapor) and air flow.

The streamline pattern of the flow upstream of such a probe is affected by the physical presence of the probe and the rate at which the sample is withdrawn. The distribution of water droplets in the stream is changed by such disturbances because relative velocities are set up in a direction transverse to the stream, causing the stream tube which enters the probe to have either too high or too low a water-air ratio, depending on the direction of the relative transverse velocity of the droplets and air upstream of the probe.

The area change of the stream tube entering the probe, however, can be controlled by varying the sample flow rate, and at a particular value of this flow rate, the area change mentioned is zero, in which case the water air ratio of the sample is taken to be truly representative of the main stream. Two techniques were developed for identifying this sampling rate, and are discussed in this report. The first method requires a direct calculation of the area change of the stream tube entering the probe, using a simplified one-dimensional analysis of the flow upstream of the probe involving the assumptions that there is no evaporation in the main stream, that the water velocity and air velocity are equal in magnitude at the probe location, and that the water droplets occupy negligible volume. The second method requires the use of a probe designed to measure the static

20526

Cambridge, Massachusetts
May 25, 1953

Professor Earl P. Millard
Secretary of the Faculty
Massachusetts Institute of Technology
Cambridge 39, Massachusetts

Dear Sir:

In accordance with the requirements of the degree of Naval Engineer, we herewith submit a thesis entitled "A Sampling Technique for the Measurement of Water-Air Ratio of a High Speed Spray-Laden Air Stream."

Respectfully,

TABLE OF CONTENTS

I Introduction

Object and Approach 1
Previous Investigations 2

II Procedure

Description of Apparatus 3
Description of Probes 10
Analytical Method 11

III Results and Discussion

Principal Results 17
Effect of Shape 24
Pressure Differential Method 26
Traverse of Stream 27

IV Conclusions 29

V Recommendations 30

VI Appendix

A-1 Symbol List 33
A-2 Supplementary Introduction 34
B-1 Calculation of Specific Humidities and Water-Air Ratios 36
B-2 Calculation of Sample Flow Rate 37
B-3 Calculation of Local Mach Number 39
B-4 Calculation of Area Ratio 42
B-5 Method of Integrating Traverse 43
C Summary of Area Ratio Calculations 45
Derived Values 46
D Sample Calculations 53
Original Data 56
Literature Citations 63

LIST OF FIGURES AND TABLES

Figures

I	Round Nose Probes	4
II	Sharp Nose Probe	5
III	Pressure Differential Probe	6
IV	Schematic Diagram	7
V	Dewcel Operating Characteristics	9
VI	Measured Water-Air Ratio vs. Sample Mass Flow	12
VII	Water-Air Ratio vs. Area Ratio	14
VIII	Pressure Differential vs. Water-Air Ratio	16
IX	Normalized Water-Air Ratio vs. Area Ratio, Round Nosed Probes	18
X, XI	Do, Sharp Nosed Probes	19
XII	Water Air Ratio vs. Area Ratio	20
XIII	Normalized Water Air Ratio vs. Pressure Difference	21
XIV	Traverse Measurement	22
XV	Recommended Probes	31

Tables

I	Comparison of Values of α^* obtained by Area Ratio and Pressure Differential Methods	23
II	Summary of Area Ratio Calculations	45
III	Derived Values	46
IV	Original Data	56

I. INTRODUCTION

The objective of this investigation was to develop a technique for measuring the water-air ratio in a high speed spray-laden air stream. The desirability of being able to evaluate the dispersion produced by atomizers injecting water into air streams has become apparent in the current investigations into the possibility of obtaining a stagnation pressure increase in a high temperature air stream by evaporative cooling [4]. Such a technique might also be useful in the evaluation of fuel injectors for ram jet engines, or in the measurement of water air ratios encountered by planes flying through clouds.

The approach employed was to withdraw a sample from the stream through a probe, and to measure its water air ratio. The crux of the problem was to insure that the sample obtained was truly representative of the stream and not in error as a result of the divergence of the water drop trajectories from the air streamlines caused by the disturbance of the flow pattern by the presence of the probe.

Two methods were employed to assure that a true sample was obtained. In the first, the upstream area of the stream tube entering the probe was calculated by a one dimensional analysis, and a true sample was inferred when this area equaled the area of the probe entrance. The second method was to measure the difference between the interior and exterior pressures just downstream of the entrance of a sharp

edged probe, a true sample being inferred when this difference is zero.

Kesler [1] investigated the use of a sampling probe to measure liquid concentration in a spray-laden air stream with velocities between 25 to 99 feet per second. He concluded that the measured ratios did not vary with sampling rate in the range of his experiments, and therefore that the collection efficiency [2] could be assumed to be one hundred per cent.

The present investigation involved air speeds of the order of magnitude of 400 feet per second. Furthermore, the authors found considerable variation of water air ratio with sampling rate, and in fact collected extensive data on this variation in the expectation that some peculiarity in the behavior of the function might provide an expeditious and positive identification of the true sample.

Other investigators [3] have approached the problem employing measurement techniques involving electrically heated resistance wire loops to measure the cooling effect of impinging water drops. Since one requirement of this system is that the surface of the wire must be able to evaporate all of the impinging water, it was felt that the technique would be unsuitable for high water air ratios. Further, mechanical strength of the wire loop is a factor which would seriously impair its use in high speed streams.

II. PROCEDURE

The experimental investigation upon which this thesis is based was carried out in an apparatus designed by Wadleigh [4] and Larson [5], and built under the sponsorship of the Aerothermopressor Project. The small scale (2-1/8 inch) subsonic aerothermopressor, which is a duct fitted with an atmospheric inlet nozzle and a diffuser exhausting to the laboratory air exhaust system, was used as a source of a high speed spray laden air stream. The water injection nozzle used for this investigation was the so-called multiple prong nozzle consisting of seven parallel tubes of 0.110 inch inside diameter arranged six on a 1-1/4 inch diameter pitch circle, one at center; and aligned with the axis of the aerothermopressor, the nozzle discharge plane being coincident with the plane of minimum bellmouth area (entrance to cylindrical test section).

The sample was withdrawn from the aerothermopressor at a point about fifteen diameters from the plane of injection by means of probes designed by the authors, (See Figures I, II, and III) and led into the humidity measuring apparatus described by Larson (op.cit.). A schematic diagram of the humidity measuring apparatus is given in Figure IV.

The sample was conducted through electrically heated piping, to minimize condensation of vapors, to the boiling water heat exchanger, the function of which was to evaporate all the water withdrawn from the airstream. A standard ASME

FIGURE I

ROUND NOSE PROBES

II & IIA

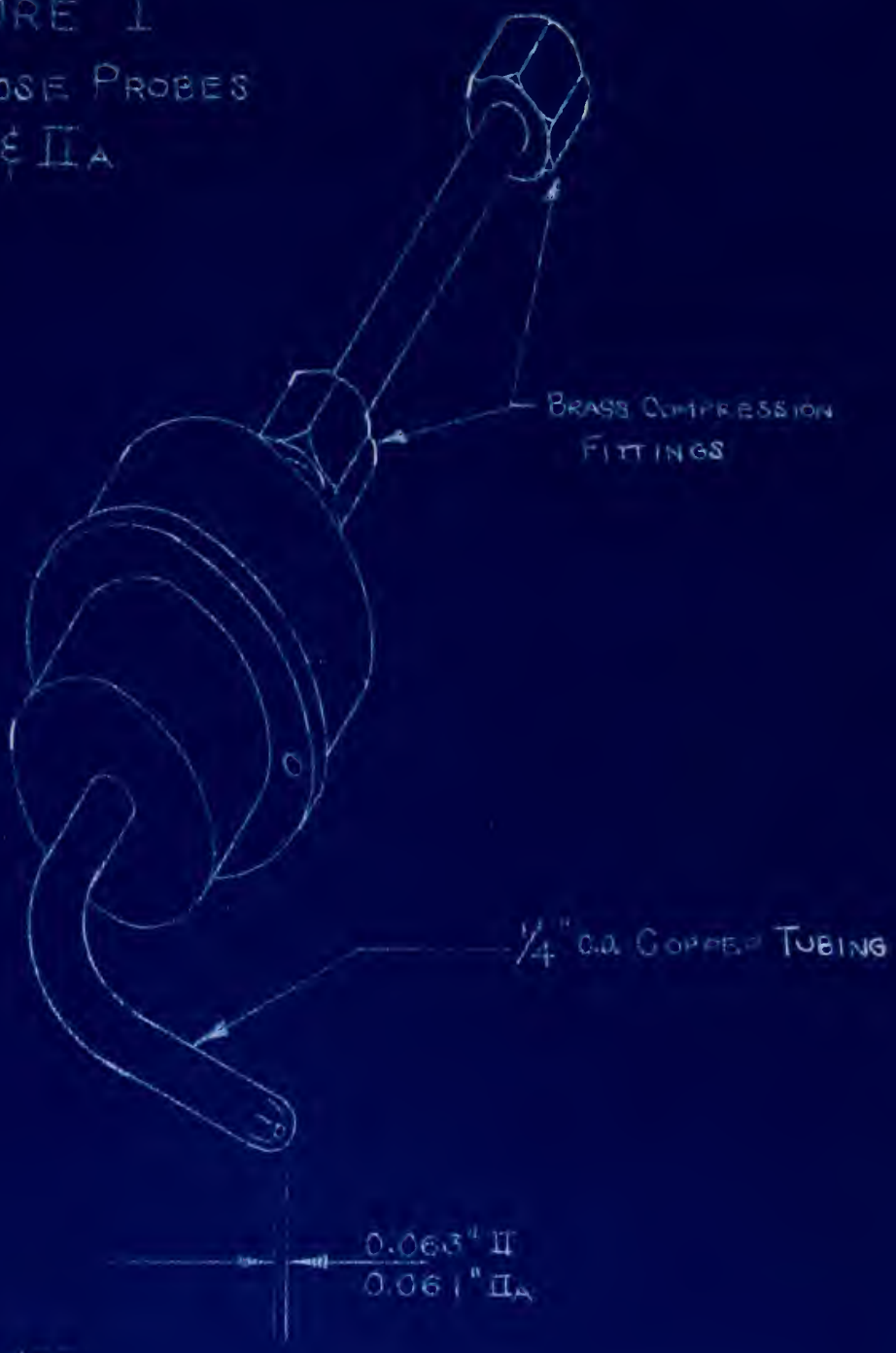

5/20/53

R.E.K. J.H.E.V.

FIGURE III

PRESSURE DIFFERENTIAL PROBE

IV

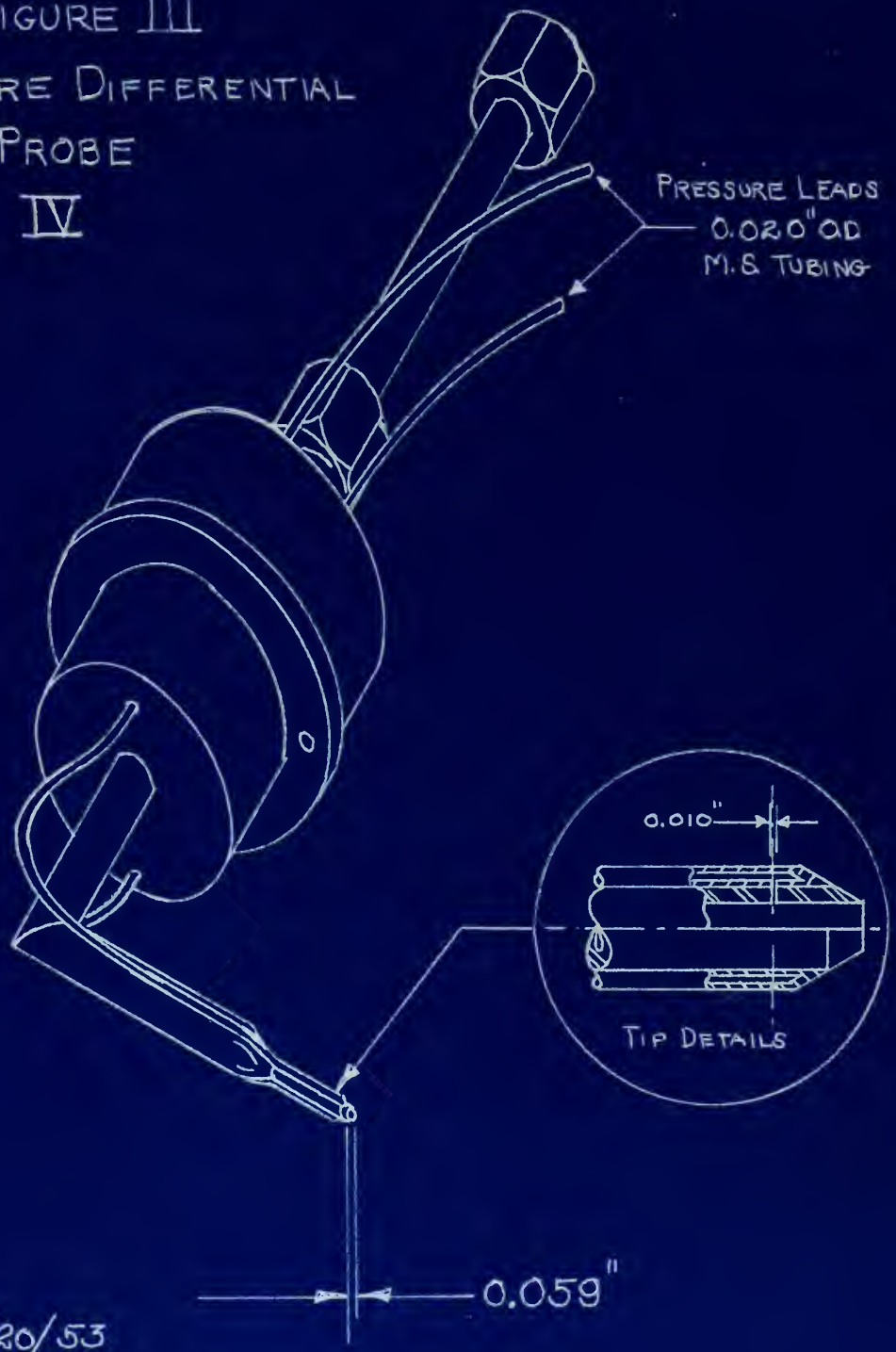

5/20/53

P.E.K. J.H.E.V.

long radius flow measuring nozzle was installed directly after this heat exchanger for the purpose of measuring the sample mass flow rate. Since the surface area of the heat exchanger was sufficiently large, it has been assumed for the purpose of this investigation that the temperature of the sample was constant at 205° F. at the inlet to the flow measuring nozzle.

The steam and water heat exchanger following the flow nozzle was intended to provide a means for controlling the temperature of the sample discharged to the sensitive element and to maintain the ambient temperature within the Dewcel chamber in the range of operation of the sensitive element. The characteristic curve of the Dewcel sensitive element is included as Figure V of this report.

The sensitive element is a "thin walled metal socket (to fit a Foxboro thermometer bulb) covered with a woven glass tape impregnated with lithium chloride. A 25 volt alternating current power supply is connected to a pair of silver wires wound over the tape. If the temperature of the Dewcel is below the equilibrium temperature, the salt absorbs moisture from the atmosphere, the conductivity of the solution on the tape between the wires increases, and the current flow increases, raising the Dewcel to equilibrium temperature. This temperature is then determined and used as a measure of the dew point temperature." *

---

*Foxboro Company Instruction Sheet 3-311, Foxboro Dew Point Measuring System, November 1950. The Foxboro Company, Foxboro, Mass.

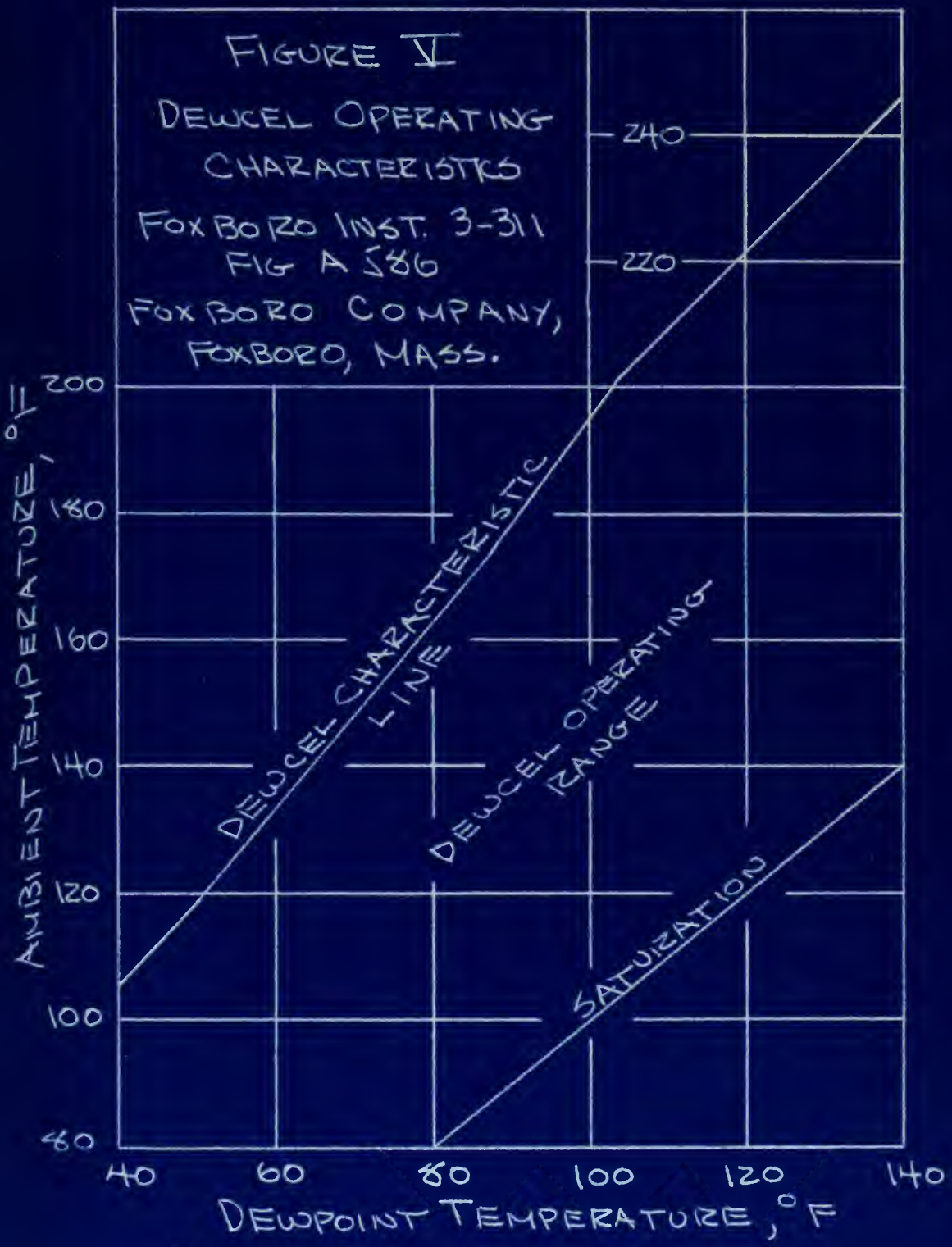

5/20/53
P.E.K.S.H.E.V.

The dew point of the sample in contact with the sensitive element was read directly on either of two remote reading gas filled thermometers, calibrated in accordance with the saturation characteristics of lithium chloride. The thermometers covered a range of dew points from 81° F. to 142° F., overlapping in the range 94° F. to 103° F.

The Dewcel chamber was a cylindrical shell connected to the sample piping and surrounded by an annular space through which the steam and water from the temperature control heat exchanger was discharged. A suction line from the sample chamber connected to the main aerothermopressor exhaust system, and the pressure in the chamber was varied from slightly below atmospheric to about 25 inches of mercury vacuum by means of a throttling valve in this line. For the sake of brevity a more complete description of the apparatus is omitted here, and the reader referred to the original work by Larson for details.

The probes used in this experimental investigation were of two general types. The first shape investigated was a round nose type having a sudden expansion just downstream of the probe entrance hole. Two such probes were tested, of slightly different hole diameters, but of external dimensions as shown in Figure I. A second shape investigated was a sharp nosed probe of stainless tubing, with a parallel section about one inch in length preceeding any expansion of the sample flow. The dimensions of this probe are given in Figure II.

A variation on the second type of probe was constructed by the Boston Naval Shipyard for the authors, which was similar in general shape to that shown in Figure II, but had in addition pressure taps arranged to read the pressures internal and external to the probe close to the entrance. The details of construction of this probe are given in Figure III.

Because of the difficulty of maintaining the pressure leads of the last probe free from water droplets, a method of periodically freeing these leads was devised. A clean air supply at about 10 pounds per square inch gage was provided by means of a reducing valve and grease trap connected to the laboratory service air supply. This low pressure air supply was connected to the pressure leads by means of commercial pyrex three way cocks, the free side of each cock being led to a differential water manometer. By careful manipulation of the valves, it was possible periodically to free the pressure leads of water by blowing them out under pressure, and thus obtain stable readings on the differential manometer.

The experimental data leads to values of specific humidity as a function of sample flow rate, the calculation of which is described in Appendices B-1 and B-2. The function is plotted in Figure VI for a representative run, with specific values of injected water-air ratio and inlet Mach Number.

It was desired to express the function of humidity against flow rate in a dimensionless form to enable the correlation of data from the various runs. For this purpose

FIGURE VI

MEASURED WATER-AIR RATIO
VS SAMPLE MASS FLOW
RUN 30a

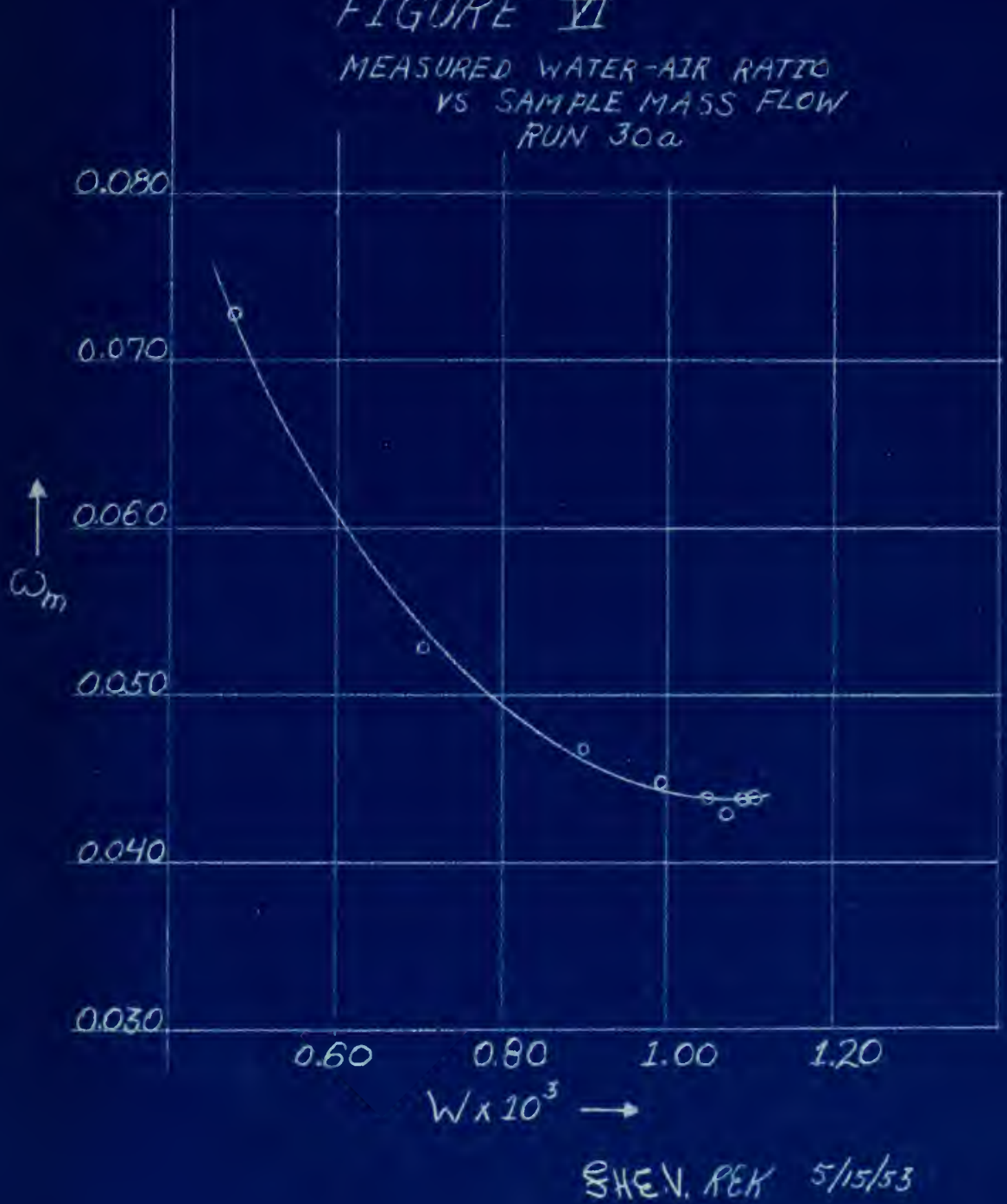

SHEV. REK 5/15/53

an area ratio was chosen which is representative of the change in cross section of the stream tube entering the probe, and is a function of the local pressure, temperature, Mach Number, the injected water-air ratio and the sample flow rate. The local Mach Number and temperature are calculated from a one-dimensional analysis, given in Appendices B-3 and B-4. In all calculations it has been assumed that the liquid entering the probe occupies negligible volume.

Within the limits of the assumptions used in obtaining the area ratio, as discussed below, the actual value of the stream water-air ratio is given by the value measured by the apparatus when the area ratio has a value of unity. This value, designated ω^*, was obtained from plots of ω, corrected for atmospheric humidity, against area ratio, representative plots being shown in Figure VII.

The alternative method of indicating the proper value of mass flow at which to measure the water air ratio of the stream is the use of the differential pressure measurements obtainable with the probe shown in Figure III. A zero differential pressure reading indicates that the velocity of the fluid entering the probe is the same as the free stream velocity at that point, hence the value of the area ratio as described above should be unity. In view of the difficulty of obtaining a zero differential pressure measurement within a reasonable time, plots of pressure differential against measured specific humidity were made, the point of zero pressure differential being interpolated to find the value

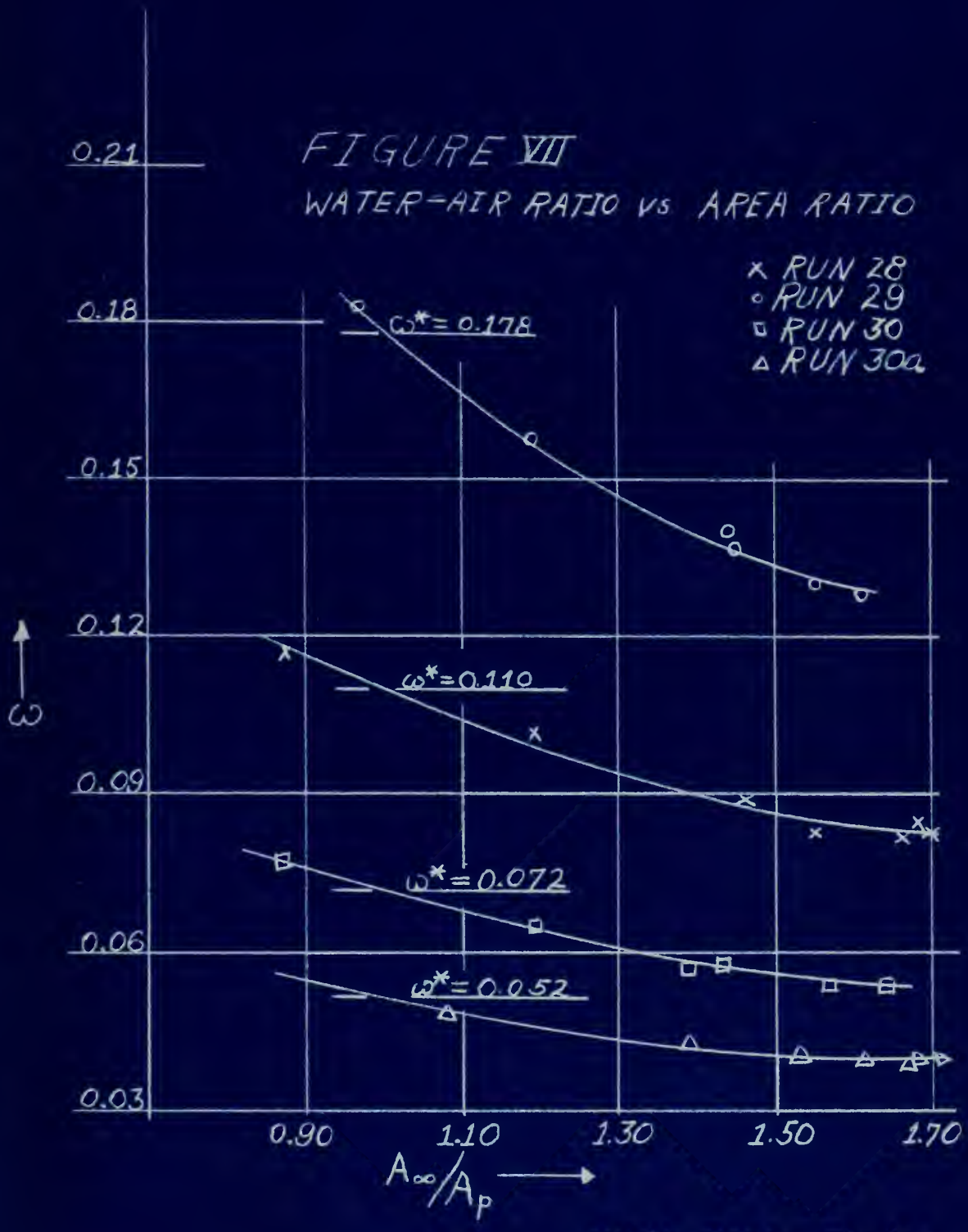
FIGURE VII
WATER-AIR RATIO vs AREA RATIO
× RUN 28
○ RUN 29
□ RUN 30
△ RUN 30a
0.21
0.18
0.15
0.12
0.09
0.06
0.03
ω
ω* = 0.178
ω* = 0.110
ω* = 0.072
ω* = 0.052
0.90
1.10
1.30
1.50
1.70
A∞/Ap
SIEV. R.E.K. 5/15/53

of ω^*. Representative plots of this form are given in Figure VIII.

An attempt was made to obtain traverse measurements of ω^* across the stream, and by integrating these points to obtain an average with which to compare the bulk average calculated from the known air mass flow and water injection rate at the inlet to the aerothermopressor. The details of this calculation are given in Appendix B-3.

FIGURE VIII

PRESSURE DIFFERENTIAL vs WATER-AIR RATIO

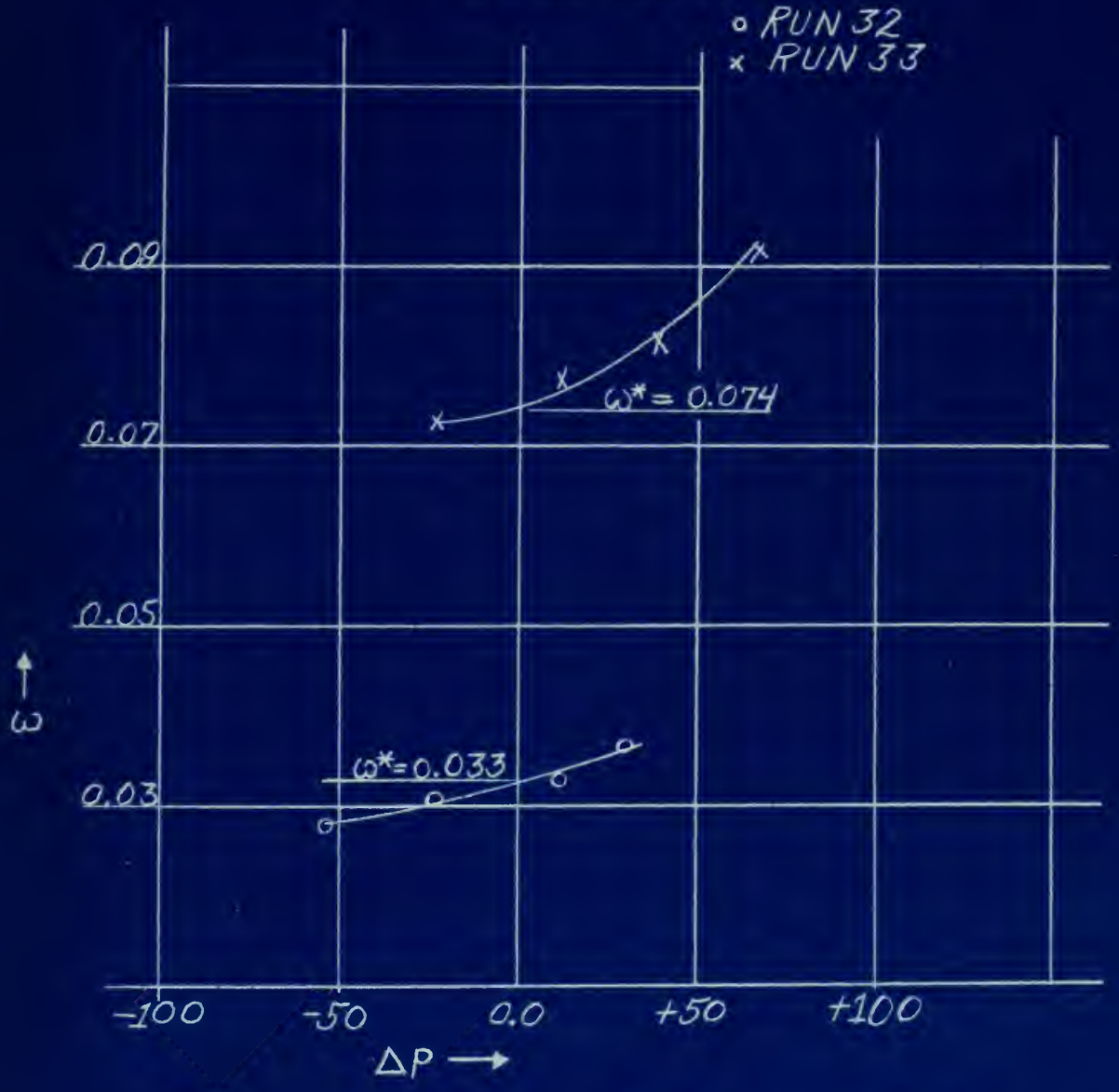

SHEV. REK 3/15/53

III. RESULTS AND DISCUSSION

The ratio of the measured humidity to the starred value, obtained as described above, was plotted as a function of area ratio, A_∞/A_p, and is presented in Figures IX, X, and XI, in the form of combined plots for all runs analyzed for each type of probe, including that one fitted for pressure measurements.

The mean lines for each type of probe are replotted on log-log scales in Figure XII, to indicate the effect of the probe shape on the results obtained.

The results obtained by differential pressure measurements with the third type probe are presented in the form of a plot of humidity ratio as a function of pressure differential, Figure XIII.

A comparison of the results obtained by the pressure differential method with those obtained by the one dimensional calculations leading to the area ratio, for the same runs as shown in Figure XI, is given in Table I.

The results of a radial traverse are presented in Figure XIV, the values of ω^* having been computed by both methods.

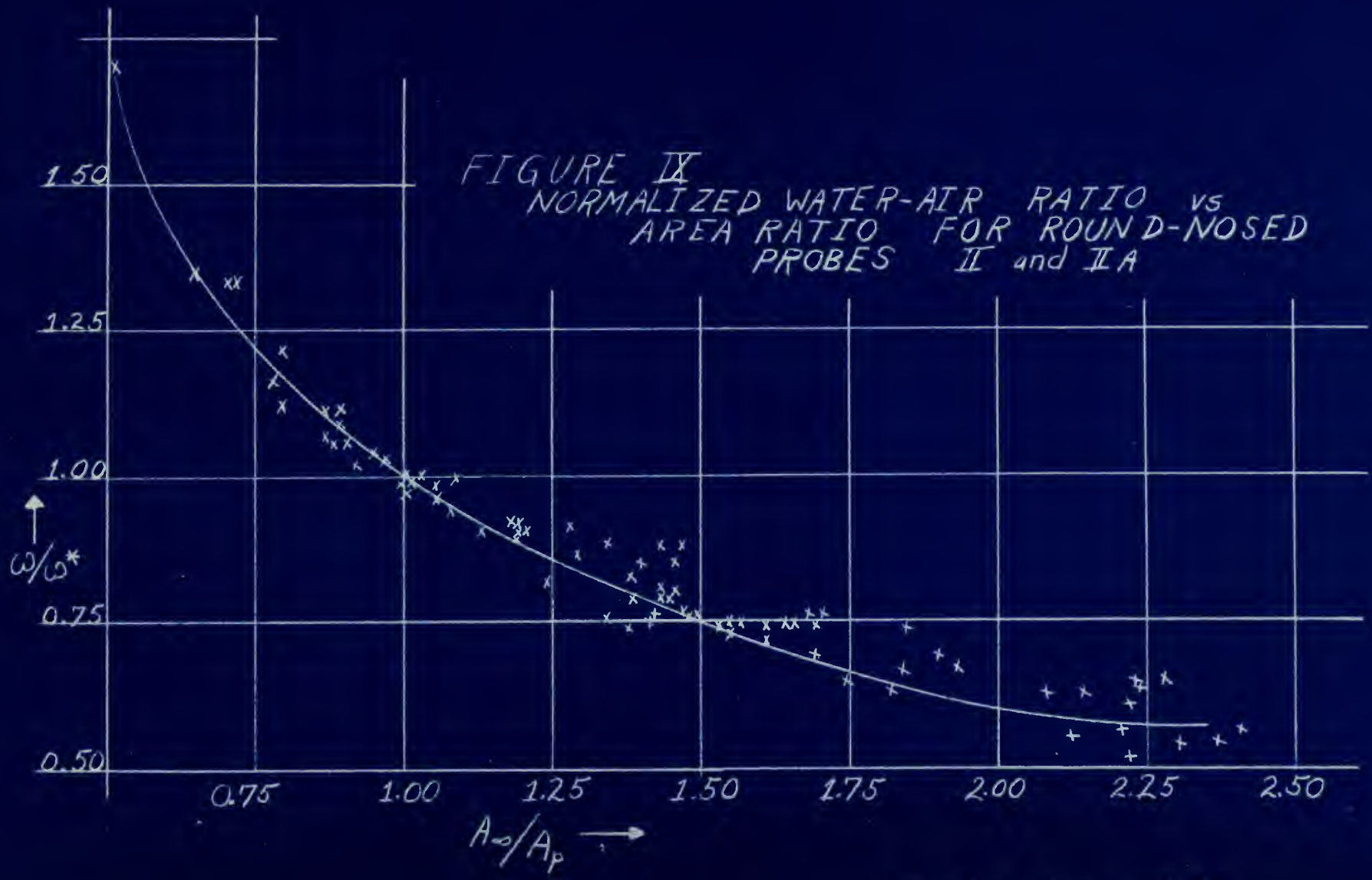

FIGURE IX
NORMALIZED WATER-AIR RATIO vs
AREA RATIO FOR ROUND-NOSED
PROBES II and IIA

SHEV. R.E.K. 5/15/53

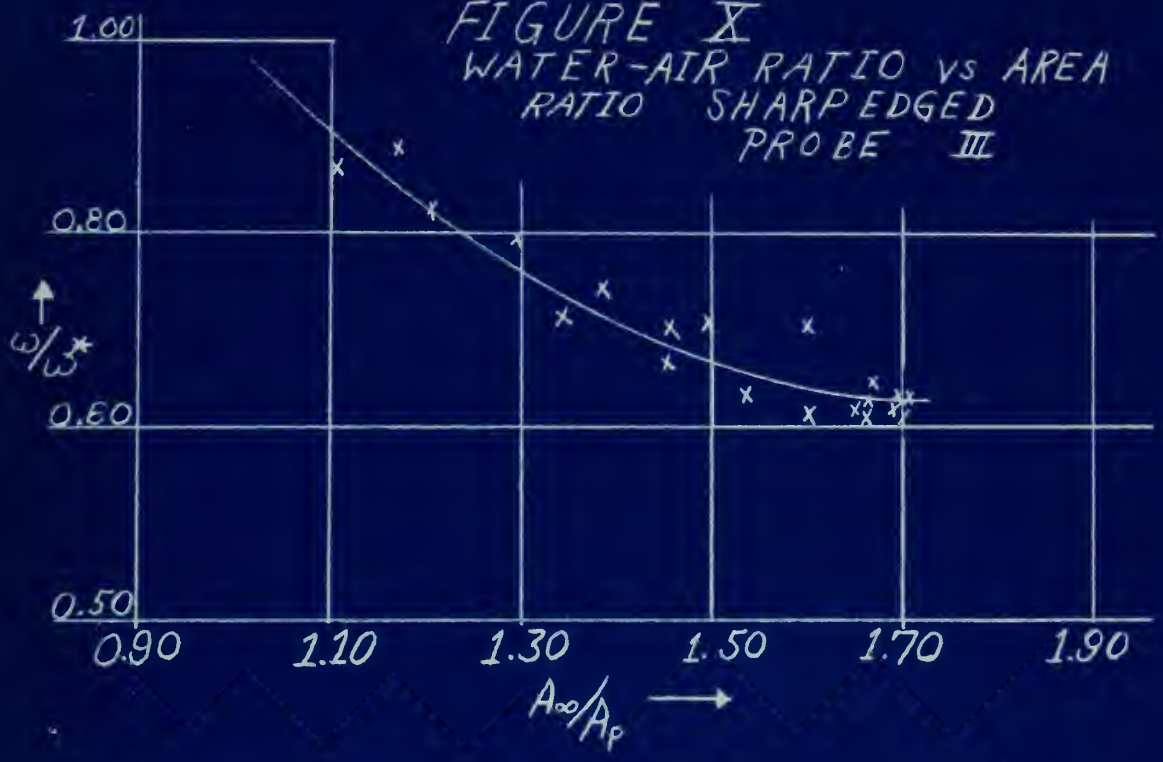

FIGURE X
WATER-AIR RATIO vs AREA RATIO SHARP EDGED PROBE III

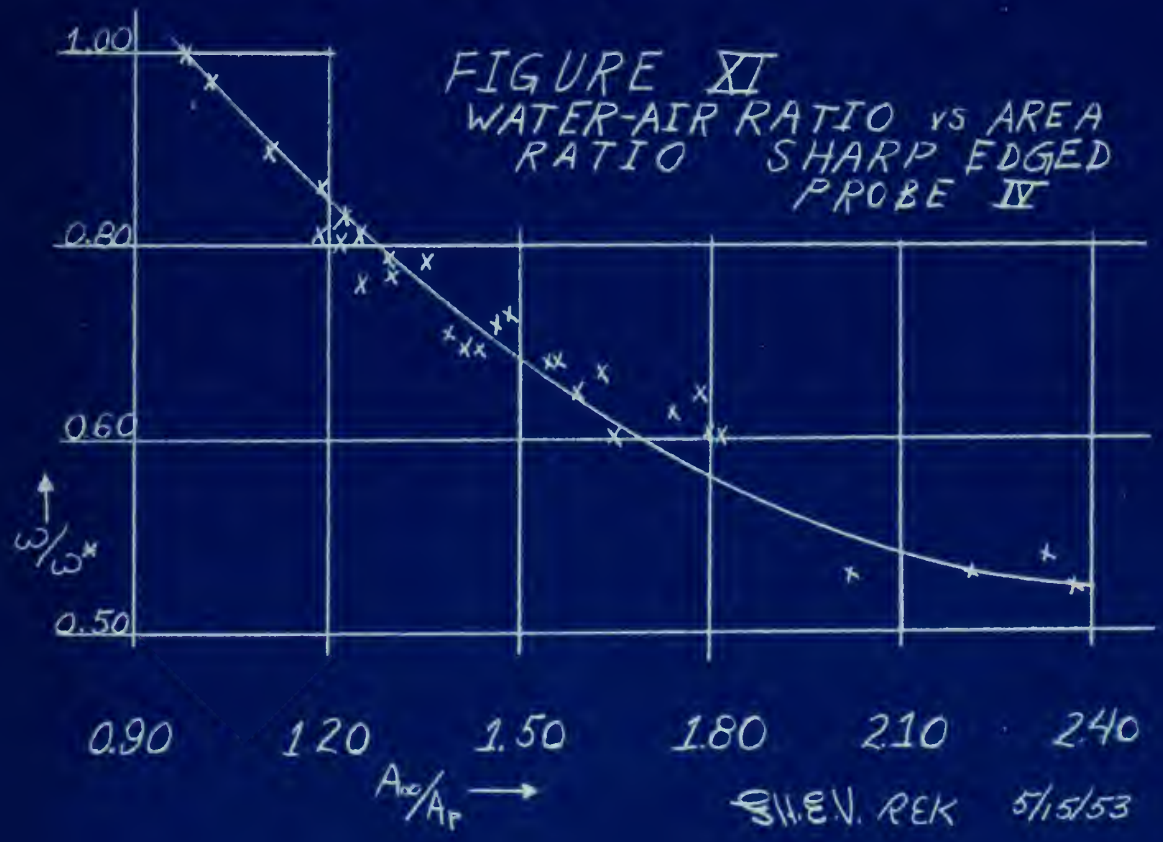

FIGURE XI
WATER-AIR RATIO vs AREA RATIO SHARP EDGED PROBE IV

S.H.E.V. REK 5/15/53

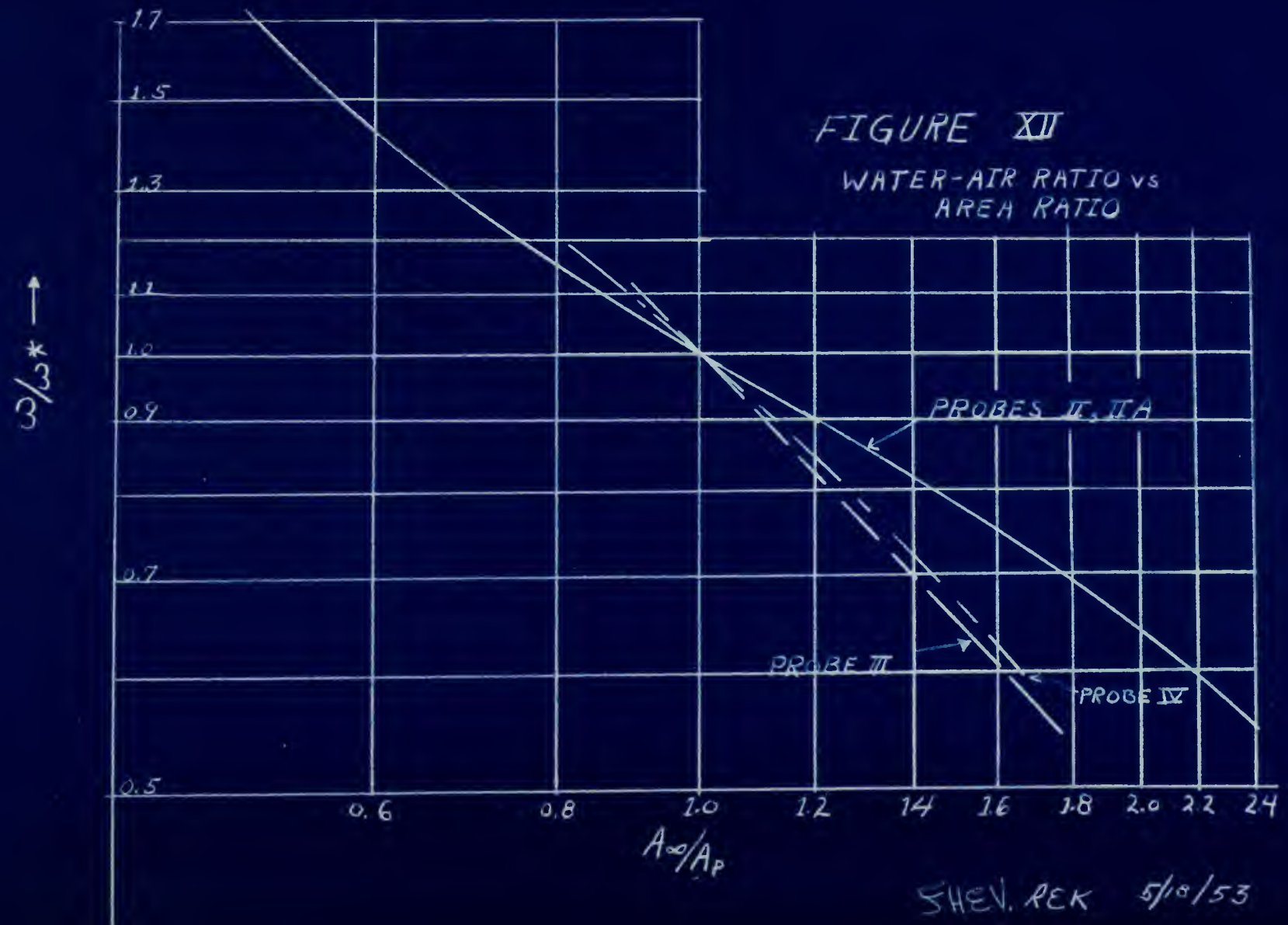
FIGURE XII
WATER-AIR RATIO vs AREA RATIO
β/β^*
1.7
1.5
1.3
1.1
1.0
0.9
0.7
0.5
0.6
0.8
1.0
1.2
1.4
1.6
1.8
2.0
2.2
2.4
A_∞/A_P
PROBES II, IIA
PROBE III
PROBE IV
SHEV. REK 5/18/53

FIGURE XIII
NORMALIZED WATER-AIR RATIO vs PRESSURE DIFFERENCE

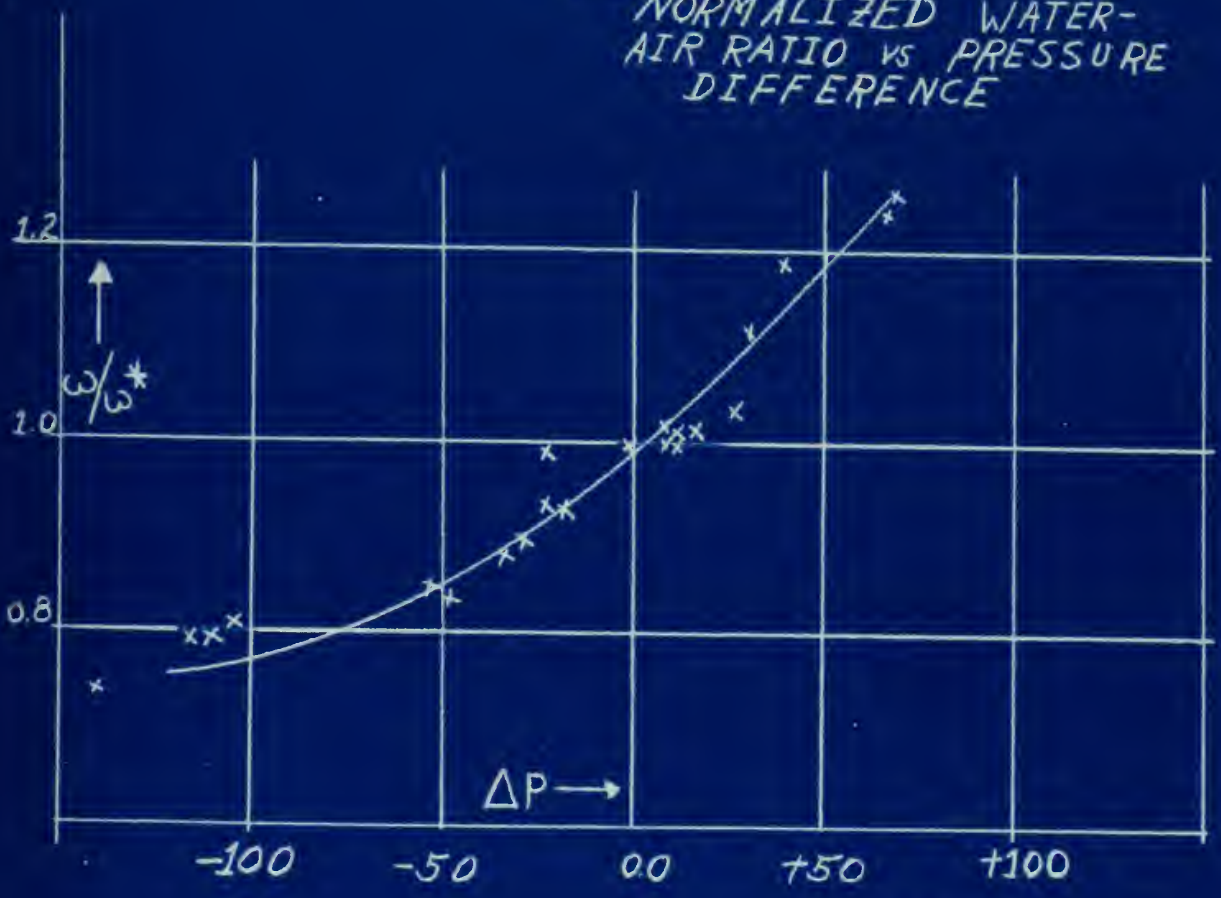

J.H.E.V. P.E.K. 5/20/53

FIGURE XIV

TRAVERSE MEASUREMENT

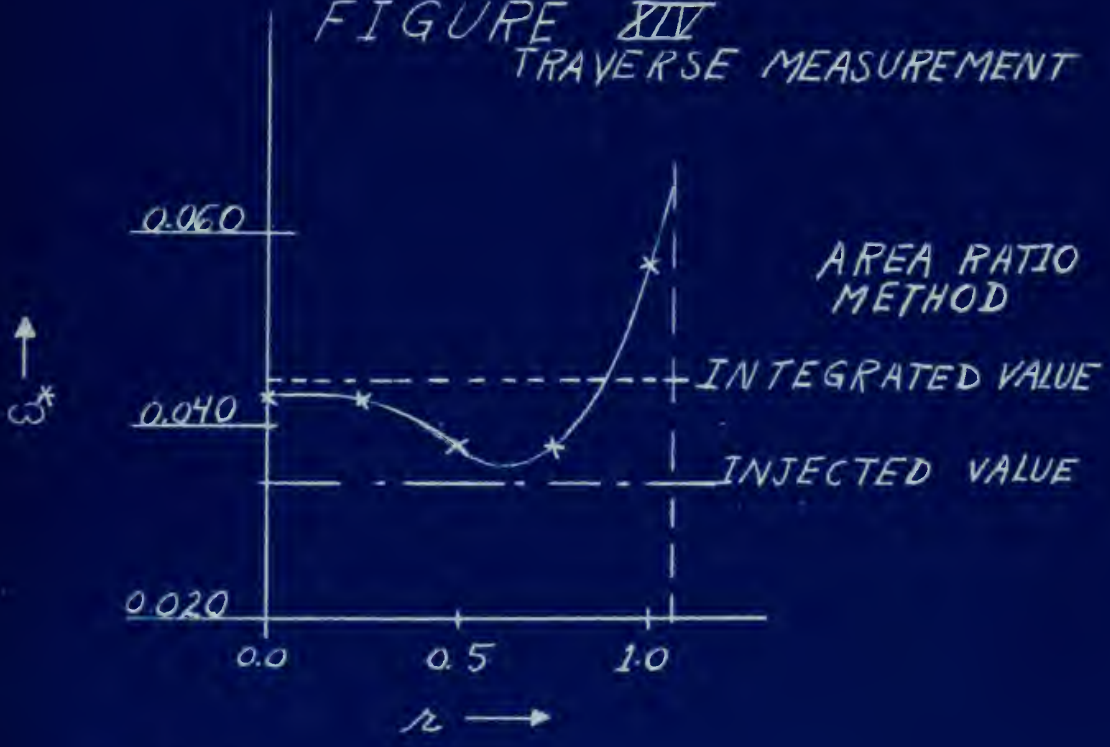

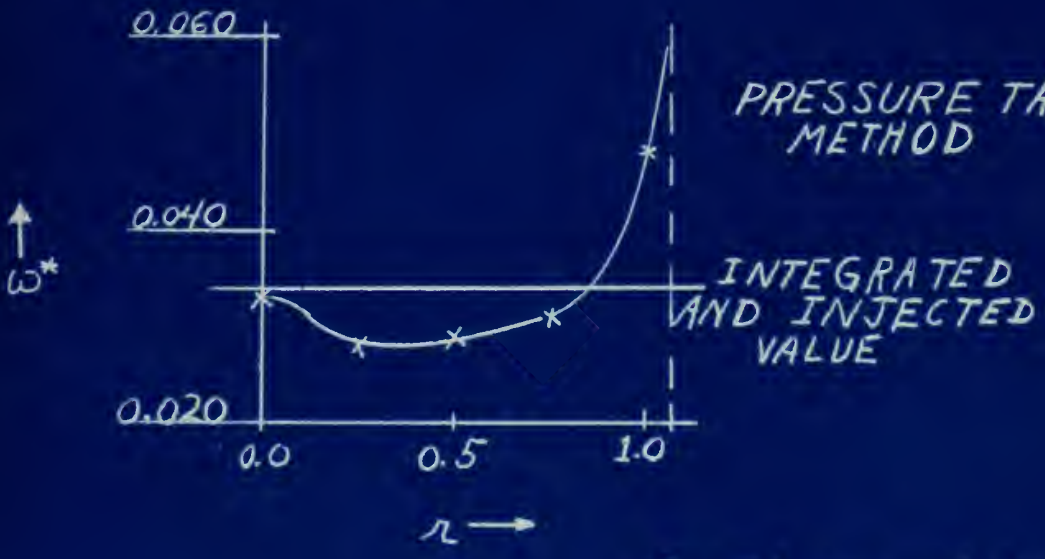

S.H.E.V. REK 5/18/53

TABLE I

COMPARISON OF VALUES OF ω^* OBTAINED BY AREA RATIO AND PRESSURE DIFFERENTIAL METHODS

Run	ω_o	M_2	ω^* By A_∞/A_p	ω^* By Δp_p	Dist. of Probe From $\mathcal{C}$
31	0.034	0.365	0.043	0.034	0"
32	0.034	0.365	0.043	0.033	0"
33	0.080	0.475	0.102	0.074	0"
34	0.034	0.365	0.043	0.028	1/4"
35	0.034	0.365	0.038	0.028	1/2"
36	0.034	0.365	0.038	0.031	3/4"
37	0.034	0.365	0.057	0.048	1"

The experimentally obtained function relating ω/ω^* and A_ω/A_p , given by Figure IX, represents data from twelve individual runs with the round nosed probes, over a range of inlet Mach Numbers from 0.24 to 0.52 and of injected water air ratio from 0.024 to 0.127 lbs. water/lbs. air. The maximum value of A_ω/A_p for individual runs is a function principally of local Mach Number, and is approximated by the value of A/A^* for one-dimensional isentropic flow corresponding to the local Mach Number. (7)

The divergence of experimental points from the mean line at high values of A_ω/A_p is expected from a consideration of the geometry of the probe and the nature of the flow pattern when a high sample rate is induced. Since there must be a considerable eddy effect under these conditions because of the bluntness of the probe profile, and therefore no opportunity for the flow to "scavenge" the face of the probe of impinged water drops: and since the pressure inside the probe is lower than the pressure on the face, there is a tendency for the impinged water to enter the probe at high flow rates, thus increasing the humidity measured by the Dewcel. At low flow rates, where the eddy effect is less prominent, such "spillover" is less likely, and in fact was not observed.

The similar plots for the sharp edged probes, Figures X and XI, evidence no such divergence from the mean line at high sampling rates. Since with this type of probe such a "spillover" effect is not to be expected, the authors reason that the effect may be ignored in striking a mean line for the round nosed probes.

Figure XII is a replot of the mean lines of Figures IX, X, and XI, showing a slight variation of slope of the curves for the three probes. Since in the opinion of the authors the first and second types represent the extreme variations of possible probe shapes, and the third type gives results falling intermediate to the other two, it is not likely that any other probe shape will produce significantly different results.

The difference in geometry of the sharp edged and blunt nosed probes is also manifested in the area ratios calculated for choking sample flow. For the blunt probe, with a sudden expansion of the sample stream after entering the probe, the area ratios at choke correspond to those for one-dimensional isentropic area change for the calculated local Mach Numbers. The sharp edged probes choke at an appreciably lower A_∞/A_p due to the effect of friction in the small diameter entrance section, and at sufficiently high Mach Numbers it is expected that choking might occur at a sampling rate corresponding to a value of A_∞/A_p less than unity.

It is readily apparent from Figure XII that there is no feature of this experimental function which lends itself to rapid determination of the value of ω^*, without recourse to calculations involving approximations as to the nature of the flow in the vicinity of the probe. In essence the results so far discussed provide a comparison procedure, but in the opinion of the authors do not contribute directly to the problem of instrumentation which is the ultimate objective of this thesis.

The pressure differential method, however, seems to the authors to have considerable promise as the basis of a useful procedure for obtaining results independent of the local pressure, temperature and Mach Number. The results of several runs using the probe designed for this method and the differential manometer and freeing system described above, are given in Figure XIII. These results indicate lower values of ω^* than those obtained from the A_ω/A_p calculation method, as summarized in Table I.

It is suspected that the size of the external pressure leads, while as small as was thought feasible to manufacture, was still large enough to disturb the flow over the outside tap. If so, the pressure indicated by the outside tap is too low. The sign of the pressure differential has been chosen in such a way that an indicated value of the external static pressure which is too low results in a value for pressure differential which is too high. Were it possible to correct the pressure differential for this effect, the disparity noted in Table I would be reduced. It is thought that a redesign of the probe, either locating the outside tap further downstream or providing internal pressure leads, would improve this condition.

In obtaining differential pressure readings, much difficulty was encountered because of excessive time lag before equilibrium of the pressure system was reached, and because of the fouling of the pressure leads with water during this time lag. The flexible tubing used in the construction of

the apparatus was too large, being chosen to fit the smallest size pyrex three way cocks available; and required a relatively large flow through the small tap openings to produce equilibrium in the system. As long as any appreciable flow through the taps is required, some trouble is to be expected with water intering the pressure leads, and was in fact encountered. It was not possible to obtain an equilibrium state in the system before the leads fouled with water, making it necessary to blow them out several times before producing two identical readings. The use of the smallest tubing and manometer commensurate with avoiding capillary effects in the manometer is recommended.

Since tightness of the system is essential, it is recommended that the use of the glass three way cocks be continued, as these can be regreased as necessary, and are known to be ground to close tolerances; but a smaller size would be desirable for the reasons stated above.

As an approximate check on the validity of the results obtained by the above methods, a traverse measurement of water air ratio across the stream was made. The details of the traverse are given in Appendix B-5, where average water-air ratios across the stream have been computed by both methods. Because of mechanical limitations, the traverse was completed across only one half of the stream, making it necessary to assume in the integration procedure that the flow was axially symmetrical. In addition the authors consider that more attention in the design of the probe

might well have been directed to insuring accurate axial alignment and transverse positioning of the probe.

While the average water-air ratio obtained from integration of the area ratio data is greater than that known to have been injected into the apparatus, and that obtained by integration of the pressure data is reasonably close to the injected value, the authors do not place sufficient faith in this traverse to regard the pressure differential method as wholly substantiated. Nor do they consider the validity of the area ratio correlation to be negated on this ground alone, except as further indication that the assumptions used in the calculations are not sufficiently precise for the development of a useful instrument.

As a final comment, we wish to point out that the shape of the experimental functions presented here is attributable only to the interaction of the liquid and gas phases in the stream. For the case of a significant amount of evaporation, the data must be interpreted as applying only to the liquid phase. Since, however, the measurements of water air ratio are eventually desired to be made in such a way that the probe produces no disturbance in the upstream flow pattern, the accuracy of measurement possible with the pressure tap method is in no way impaired.

IV. CONCLUSIONS

The area ratio method is not satisfactory for practical instrumentation, but offers a comparison technique for evaluating other methods.

The pressure tap method, although obviously not yet raised to a satisfactory level of precision, offers the best promise for development of a successful instrument.

V . RECOMMENDATIONS

It is recommended that the emphasis in further research be placed on the development of a probe employing the pressure differential technique as a means of indicating the desired flow conditions for measuring the stream water-air ratio. Recommended probe configurations are given in Figure XV, where it will be noticed the major consideration has been to improve the shape in the region of the external pressure opening to avoid incorrect indications of external static pressure. The length of the parallel entrance section should be kept as short as possible in order to avoid difficulties with choking due to friction.

FIGURE XV

RECOMMENDED PROBES

5/20/53
R.E.K. J.H.C.V.

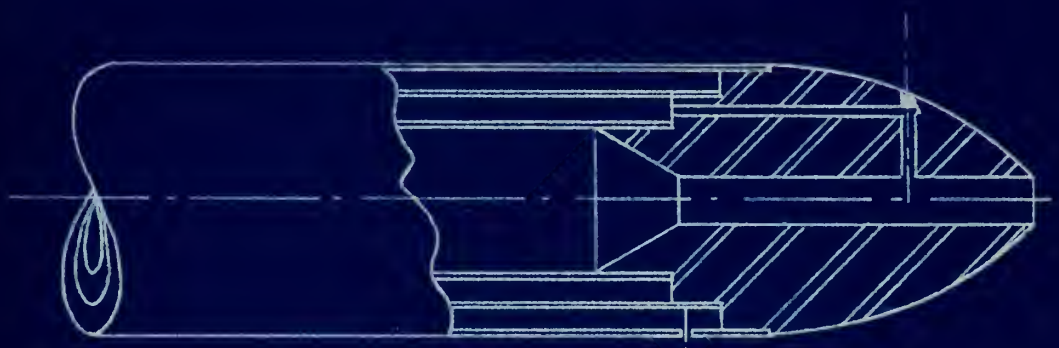

THREE CONCENTRIC TUBES WELDED TO TIP
PORTED AS SHOWN

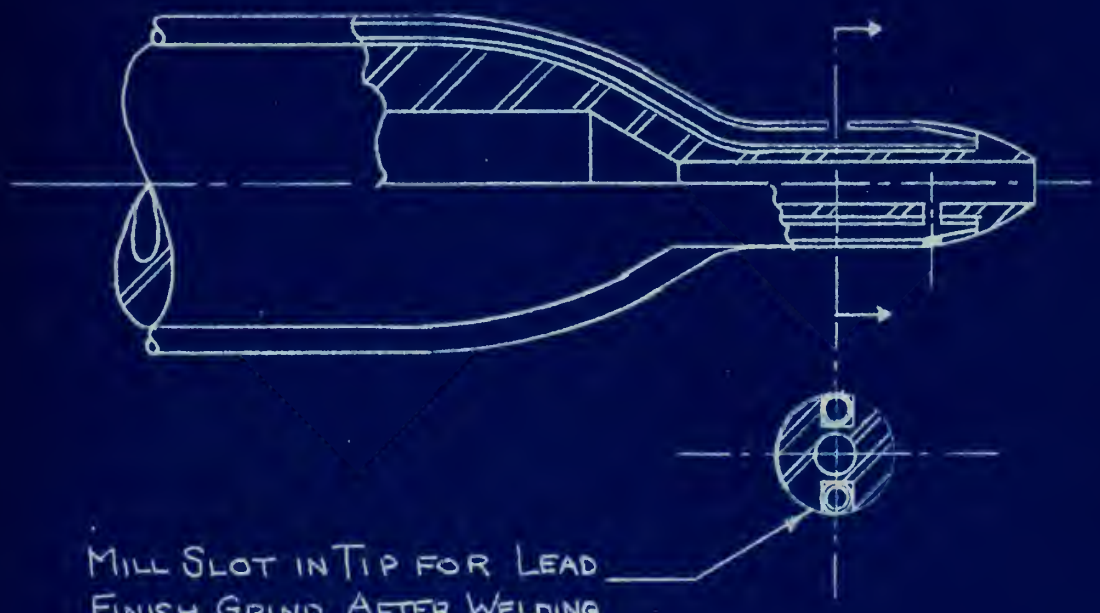

VI. APPENDIX

APPENDIX A-1

List of Symbols used in the text

A - Area, inches^2

M - Mach Number, dimensionless

P - Pressure, centimeters of mercury

ΔP - Pressure differential, centimeters of water

Rot- Refers to scale reading of Schutte and Koerting rotameter

T - Temperature, ^oF abs.

V - Velocity, feet/second

W - Total sample flow rate, pounds/second

w - Mass flow rate of gas phase, pounds/second

ρ - Mass density, pound seconds^2/feet^4

ω - Specific Humidity, pounds water/pound air

ω_o - Average injected water-air ratio

ω^* - Actual value of stream water-air ratio

Subscripts

o - Refers to stagnation condition

1 - Refers to conditions at plane of injection

2 - Refers to local stream conditions at probe location

∞ - Refers to conditions in stream upstream of probe

p - Refers to probe

a - Refers to atmospheric conditions

m - Refers to measured value

d - Refers to conditions in Dewcel

n - Refers to conditions at flow measuring nozzle

APPENDIX A-2

Supplementary Introduction

In undertaking the task of obtaining a satisfactory instrument for the measurement of the water-air ratio of a high velocity air stream, it was thought, on the basis of qualitative reasoning, that the shape of the curves of ω vs. flow rate for any shape of probe would show a point of inflection near the sample flow rate at which a true sample would be obtained. The definition implied by a "true sample" is that the effect of the probe on the stream tube which enters it is nil, so that there is no relative motion of the liquid droplets and the air in this stream tube. Furthermore, it was expected that the rate of change of measured humidity with sample flow rate would be zero or nearly so in this region.

By testing two probes of widely different shape, it was hoped that the effect sought would be found to be influenced by the shape, and that a reliable measuring system might be built around this characteristic of the flow, the ultimate shape being chosen so as to make the inflection point most prominent.

The shape of the experimental curves shown in Figures IX, X, and XI does not bear out the qualitative picture given above. Furthermore, the shape of the curves for the blunt nose and sharp nose probes is much the same, indicating that there is little chance of any intermediate probe shape exhibiting such well defined features of the experimental function as are necessary to the development of an engineering instrument on this principle.

The measurement of the external and internal static pressures has been suggested by other researchers and was used in this case as an alternative method for indicating a true sample. In principle, however, the basic essential of the problem is the necessity of withdrawing a sample from the high speed airstream in such a way as not to disturb the flow of gas and liquid droplets upstream of the sampling element. Since any probe will cause a disturbance of the upstream flow, there exists the necessity of controlling the nature of the disturbance, and the means chosen to do so here was to vary the amount of sample withdrawn. The problem was thus reduced to that of how to determine which sample flow rate is the correct one, and a technique for answering this question was the principal objective of this thesis.

APPENDIX B-1

Calculation of Specific Humidities and Water-Air Ratios

The injected water-air ratio ω_o was calculated from the several curves given by Wadleigh [1] for the 21/8 inch subsonic aerothermopressor. The inlet Mach Number and air mass flow rate are given by a one-dimensional analysis as functions of the pressure ratio $\frac{P_{oa} - P_1}{P_{oa}}$, corrected for the effect of the water injection nozzle by means of an auxiliary correction curve applying to the particular injector used. The injected water rate was taken from calibration curves for the Schutte and Koerting Rotameter used. The value of ω_o used in these calculations was given by the ratio w_{se}/w_{oa} obtained from the above quantities.

The specific humidity of the sample in the dewcel chamber was calculated from the measured pressure and dew point temperature by use of the Gibbs-Dalton rule for mixtures and the definition of the dew-point temperature. The partial pressure of water vapor in the mixture is given by the saturation pressure corresponding to the dew-point temperature, and the partial pressure of air calculated from the rule that the sum of the partial pressures of the constituent gases is equal to the measured total pressure.

Hence

$$\omega \equiv w_{se}/w_{oa} = \frac{R_a P_s}{R_s P_a} = \frac{W_s}{W_a} \frac{P_s}{P_a}$$

$$= 0.622 \frac{P_s}{P_a}$$ for water vapor and air, since the temperature of the mixture is assumed uniform.

APPENDIX B-2

Calculation of Sample Flow Rate

The sample flow rate was measured by the use of a standard ASME long radius flow nozzle with nozzle throat taps, of throat diameter 0.100 inches, installed in the 0.250 inside diameter tubing immediately downstream of the boiling water heat exchanger.

Since the sample humidities involved in these experiments were sufficiently low to allow treatment of the mixture as if it were air for the purpose of computing specific heats and molecular weight, the formulae given below for air [6] were considered adequate for the purpose. The approach velocity correction was considered negligible in this case, and only static pressures measured.

The variation in the nozzle discharge coefficient, from minimum to maximum flow rates used, was predicted from the data of (9) to be from 0.88 to 0.92, for Reynolds' Numbers based on diameter from about 2,000 to 8,000. In view of the uncertainty of the other assumptions made leading to the computed values of area ratio from measured data, it was considered sufficiently accurate to use a uniform coefficient of discharge of 0.90 for all calculations.

In addition, it has been assumed that the sample temperature entering the nozzle was 205°F for all flow conditions.

For Δp between 10 percent and 50 percent of inlet

pressure, the flow rate through a standard nozzle is given by [6] as

$$W = 0.46627\, C D^2 \sqrt{\frac{\Delta p_t}{T_1}\left(p_2 - 0.075\,\Delta p_t\right)} \qquad \text{for air}$$

or, for Δp and p_2 in centimeters of mercury, and other values as given above,

$$W = 0.5463 \times 10^{-4} \sqrt{\Delta p_u \left(p_u - 0.075\,\Delta p_u\right)}$$

For Δp less than 10 percent of the inlet pressure,

$$W = 0.45596\, C D^2 \sqrt{\frac{p_2 \Delta p}{T_1}}$$

or for Δp and p_2 in centimeters of mercury, and other values as given above,

$$W = 0.5794 \times 10^{-4} \sqrt{p_u \Delta p_u}$$

APPENDIX II-3

Calculation of Local Mach Number M_2

The local Mach Number M_2 was calculated from a one-dimensional analysis of a discontinuity using the control volume shown below:

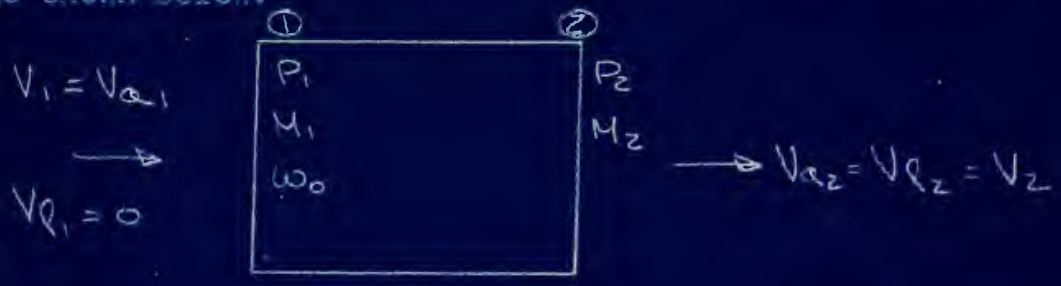

It is assumed that: 1) The water injection velocity is negligible

2) The liquid velocity and gas velocity are equal at section 2.

3) The flow is adiabatic

4) There is no evaporation of liquid in the test section.

From the Perfect Gas Rule (Equation of State)

$$\frac{P_2}{P_1} = \frac{\rho_2}{\rho_1}\frac{T_2}{T_1} \qquad (1)$$

From the Condition of Continuity

$$\omega_a/A = \rho_1 V_1 = \rho_2 V_2 \qquad (2)$$

The Steady Flow Energy Equation

$$C_p T_0 = C_p T_1 + \frac{V_{a_1}^2}{2} = C_p T_2 + \frac{V_{a_2}^2}{2} + \omega_0 \frac{V_{\ell_2}^2}{2} \qquad (3)$$

Definition of M

$$M = V/c = V/\sqrt{KRT} \tag{4}$$

Substituting (4) in (3) and noting that $\frac{KR}{C_p} = K-1$

$$T_0 = T_1\left(1 + \frac{K-1}{2} M_1^2\right) = T_2\left[1 + (1+\omega_0)\frac{K-1}{2} M_2^2\right] \tag{5}$$

Substituting (2) in (1) and using (3) and (5)

$$\frac{P_2}{P_1} = \frac{M_1}{M_2}\sqrt{\frac{1 + \frac{K-1}{2} M_1^2}{1+(1+\omega_0)\frac{K-1}{2} M_1^2 \left(\frac{M_2}{M_1}\right)^2}} \tag{6}$$

Solving for $\left(\frac{M_2}{M_1}\right)^2$

$$\left(\frac{M_2}{M_1}\right)^2 = \frac{-1 \pm \sqrt{1 + 4C_1C_2^2}}{2C_1} \tag{7}$$

Where

$$C_1 = \left[(1+\omega)\frac{K-1}{2} M_1^2\right] \tag{7a}$$

and

$$C_2 = \left[1 + \frac{K-1}{2} M_1^2\right]\left(P_1/P_2\right)^2 \tag{7b}$$

Hence

$$\frac{M_2}{M_1} = \sqrt{\frac{-1 + \sqrt{1+4C_1C_2^2}}{2C_1}}$$

where the positive sign is taken under the radical, since the negative yields a value of M_2 without physical meaning. The local Mach Number is thus calculated approximately as a function of the inlet Mach Number and the ratio of inlet pressure to local pressure.

APPENDIX B-4

Calculation of Area Ratio A_∞/A_p

The parameter chosen to normalize the flow function is derived from the following considerations:

The Condition of Continuity:

$$w_a/A = \rho V \tag{1}$$

The Definition of M

$$M = V/c = V/\sqrt{kRT} \tag{2}$$

The Perfect Gas Rule (Equation of State)

$$p = \rho RT \tag{3}$$

Hence

$$A_\infty/A_p = \frac{w_a}{A_p}\frac{\sqrt{T_2}}{\sqrt{k/R}\, p_2 M_2} \tag{4}$$

or

$$A_\infty/A_p = 5.64\ \frac{w_a}{A_p}\left[\frac{\sqrt{T_2}}{p_2 M_2}\right]$$

for p_2 in centimeters of mercury and w_a in pounds per second (equal to $W/(1+\omega)$ since the liquid entering the probe is assumed to occupy negligible volume.)

Note that A_∞ and A_2 are considered to be identical, since the point of measurement of local pressure was chosen sufficiently far upstream of the probe as to be unaffected by its presence, the condition under which the subscript is generally applied.

APPENDIX B-1

Method of Integrating Traverse Measurements

Traverse measurements were made at five positions, centerline and at each succeeding quarter of an inch, using both the area ratio and pressure differential technique. The results are plotted in Figure XIV.

To obtain an average water air ratio to compare with the known injection the following definition was used:

$$\omega_{avg_D} = \frac{\int (\rho V)\, \omega^* \, dA}{\int (\rho V)\, dA} \qquad (1)$$

The product ρV was assumed constant across the section, reducing (1) to:

$$\omega_{avg_D} = \frac{\int \omega^* dA}{\int dA} = \frac{\int_0^{r_0} r\omega^* dA}{r_0^2/2} \qquad (1b)$$

The numerator of this expression was evaluated out to a radius of one inch by applying Simpson's Rule for numerical integration with ten ordinates. The value of ω^* at radii greater than one inch is in question, since for a wet wall ω^* becomes infinite at the wall. In evaluating the integral, it was assumed that the curve of ω^* could be faired into a straight line extending from $r = 1.0$ to $r = r_0$. The contribution of this portion of the integral was computed by using a mean value of the product $r\omega^*$.

APPENDIX C

TABLE II

SUMMARY OF AREA RATIO CALCULATIONS

Run	Probe	Date	M_1	ω_o	M_2	T_o	T_2	A_o/W_o
14	II	3/25	0.270	0.036	0.279	510	502	6.37
15	II	3/27	0.243	0.084	0.249	506	500	7.15
16	II	3/28	0.240	0.125	0.251	507	498	7.05
17	II	3/28	0.420	0.024	0.455	507	486	4.25
18	II	3/28	0.420	0.050	0.457	507	485	4.22
19	II	3/29	0.415	0.079	0.473	503	480	4.15
20	II	3/29	0.520	0.043	0.640	503	464	3.36
22	IV	3/29	0.242	0.083	0.253	503	496	6.95
23	III	3/30	0.250	0.038	0.258	507	500	6.95
24	III	3/30	0.250	0.080	0.258	507	500	6.95
25	III	3/30	0.250	0.127	0.258	507	499	6.95
27	IIA	4/7	0.485	0.048	0.582	507	472	3.61
28	IIA	4/7	0.343	0.077	0.372	511	495	5.00
29	IIA	4/8	0.343	0.120	0.371	511	496	5.01
30	IIA	4/8	0.343	0.048	0.372	511	496	5.02
30a	IIA	4/8	0.343	0.034	0.372	511	496	5.02
31	IV	4/17	0.345	0.034	0.367	511	497	5.09
32	IV	4/20	0.345	0.034	0.365	505	492	5.10
33	IV	4/20	0.420	0.080	0.475	505	481	4.21
34	IV	4/20	0.345	0.034	0.365	505	492	5.10
35	IV	4/20	0.345	0.034	0.365	505	492	5.10
36	IV	4/20	0.345	0.034	0.365	505	492	5.10
37	IV	4/20	0.345	0.034	0.365	505	492	5.10

TABLE III

DERIVED VALUES

	ω_m	ω	$W \times 10^3$	$w \times 10^3$	A_e/A_p	W/W^*
Run 14 3/25 $A_p = 3.00 \times 10^{-3}$ $\omega^* = 0.046$	0.039	0.031	0.895	0.867	1.84	0.673
	0.037	0.029	1.010	0.984	2.08	0.630
	0.037	0.029	1.050	1.022	2.14	0.630
	0.036	0.028	1.074	1.046	2.22	0.606
	0.032	0.024	1.074	1.049	2.22	0.521
	0.039	0.031	0.940	0.911	1.932	0.674
	0.040	0.032	0.825	0.798	1.692	0.695
	0.050	0.042	0.630	0.604	1.280	0.912
	0.043	0.035	0.722	0.698	1.482	0.760
	0.055	0.047	0.453	0.434	0.920	1.021
	0.058	0.050	0.454	0.423	0.897	1.086
Run 15 3/27 $A_p = 3.00 \times 10^{-3}$ $\omega^* = 0.092$	0.066	0.060	0.773	0.730	1.740	0.651
	0.070	0.064	0.849	0.797	1.900	0.695
	0.066	0.060	0.993	0.939	2.23	0.651
	0.074	0.068	0.826	0.774	1.84	0.738
	0.079	0.073	0.654	0.609	1.45	0.793
	0.095	0.089	0.483	0.445	1.060	0.966
	0.066	0.060	0.983	0.936	2.23	0.651
	0.066	0.060	1.011	0.956	2.28	0.651
Run 16 3/28 $A_p = 3.00 \times 10^{-3}$ $\omega^* = 0.156$	0.091	0.086	0.977	0.900	2.12	0.551
	0.104	0.099	0.850	0.774	1.82	0.634
	0.124	0.119	0.702	0.629	1.48	0.762
	0.092	0.088	1.020	0.939	2.21	0.564
	0.089	0.084	1.067	0.983	2.31	0.538
	0.090	0.085	1.093	1.009	2.37	0.545
	0.093	0.088	1.112	1.023	2.41	0.564

TABLE III (Cont.)

	ω_m	ω	$W \times 10^3$	$w \times 10^3$	$\Lambda_\omega / \Lambda_p$	ω/ω^*
	0.035	0.030	1.063	1.034	1.470	0.883
	0.034	0.029	1.057	1.029	1.460	0.851
Run 17	0.034	0.029	1.010	0.984	1.398	0.851
3/28	0.035	0.030	0.973	0.944	1.340	0.883
$A_p = 3.00 \times 10^{-3}$	0.035	0.030	0.872	0.847	1.201	0.883
$\omega^* = 0.034$	0.039	0.034	0.750	0.725	1.030	1.000
	0.043	0.036	0.638	0.615	0.874	1.116
	0.031	0.026	1.079	1.050	1.490	0.764
	0.051	0.046	0.476	0.455	0.646	1.350
	0.087	0.082	0.800	0.554	0.778	1.170
Run 18	0.073	0.068	0.765	0.716	1.007	0.970
3/28	0.075	0.070	0.765	0.715	1.006	1.000
$A_p = 3.00 \times 10^{-3}$	0.070	0.065	0.894	0.839	1.180	0.928
$\omega^* = 0.070$	0.066	0.061	0.975	0.918	1.290	0.870
	0.067	0.062	1.082	1.019	1.431	0.885
	0.136	0.131	0.776	0.686	0.950	1.047
Run 19	0.113	0.113	0.912	0.820	1.135	0.903
3/29	0.108	0.103	0.991	0.898	1.243	0.823
$A_p = 3.00 \times 10^{-3}$	0.100	0.095	1.063	0.973	1.347	0.760
$\omega^* = 0.125$	0.097	0.092	1.089	0.995	1.379	0.736
	0.099	0.094	1.120	1.024	1.419	0.752
	0.102	0.097	1.129	1.029	1.423	0.768

TABLE III (Cont.)

	ω_m	ω	$\bar{w}x10^3$	$wx10^3$	A_ω/A_p	ω/ω^*
Run 20 3/29 $A_p = 3.00 \times 10^{-3}$ $\omega^* = 0.065$	0.078	0.073	0.760	0.709	0.794	1.120
	0.084	0.079	0.761	0.706	0.791	1.220
	0.078	0.073	0.859	0.799	0.895	1.120
	0.074	0.069	0.865	0.809	0.906	1.060
	0.069	0.064	0.946	0.889	0.996	0.985
	0.069	0.064	1.004	0.943	1.058	0.985
	0.070	0.065	1.038	0.975	1.093	1.000
Run 22 3/29 $A_p = 2.74 \times 10^{-3}$ $\omega^* = 0.060$	0.042	0.037	0.975	0.941	2.39	0.616
	0.044	0.039	0.946	0.913	2.32	0.650
	0.043	0.038	0.901	0.871	2.21	0.634
	0.043	0.038	0.824	0.795	2.02	0.634
	0.049	0.044	0.737	0.706	1.792	0.734
	0.055	0.050	0.611	0.582	1.478	0.834
Run 23 3/30 $A_p = 2.74 \times 10^{-3}$ $\omega^* = 0.060$	0.050	0.044	0.660	0.631	1.600	0.710
	0.046	0.040	0.687	0.660	1.670	0.646
	0.045	0.039	0.696	0.670	1.696	0.630
	0.045	0.039	0.698	0.673	1.704	0.630
	0.044	0.038	0.696	0.671	1.700	0.613
	0.050	0.044	0.617	0.591	1.497	0.710
	0.052	0.046	0.562	0.537	1.384	0.742
	0.061	0.055	0.490	0.464	1.173	0.887

TABLE III (Cont.)

	ω_m	ω	$Wx10^3$	$wx10^3$	A_w/A_p	ω/ω^*
Run 24	0.110	0.104	0.486	0.440	1.114	0.872
3/30	0.081	0.075	0.654	0.608	1.540	0.636
$A_p=2.74 \times 10^{-3}$	0.080	0.074	0.705	0.656	1.661	0.627
$\omega^* = 0.118$	0.079	0.073	0.711	0.653	1.654	0.620
	0.079	0.073	0.720	0.670	1.697	0.620
	0.090	0.084	0.575	0.530	1.341	0.713
	0.088	0.082	0.563	0.520	1.317	0.695
Run 25	0.145	0.139	0.542	0.476	1.207	0.826
3/30	0.124	0.118	0.641	0.575	1.457	0.702
$A_p=2.74 \times 10^{-3}$	0.118	0.112	0.638	0.574	1.452	0.666
$\omega^* = 0.168$	0.109	0.103	0.698	0.631	1.600	0.613
Run 27	0.084	0.078	1.010	0.937	1.085	0.939
4/7	0.086	0.080	0.936	0.869	1.006	0.976
$A_p=3.12 \times 10^{-3}$	0.096	0.090	0.835	0.766	0.889	1.097
$\omega^* = 0.082$	0.115	0.109	0.670	0.605	0.701	1.330
	0.146	0.140	0.496	0.435	0.504	1.710

TABLE III (Cont.)

	ω_m	ω	$Wx10^3$	$wx10^3$	A_∞/A_p	ω/ω^*
	0.091	0.085	1.139	1.049	1.680	0.773
Run 28	0.089	0.083	1.148	1.059	1.698	0.755
4/7	0.088	0.082	1.120	1.034	1.660	0.746
$A_p = 3.12 \times 10^{-3}$	0.089	0.083	1.046	0.965	1.548	0.755
	0.095	0.089	0.991	0.911	1.461	0.809
$\omega^* = 0.110$	0.108	0.102	0.817	0.741	1.189	0.927
	0.123	0.117	0.642	0.548	0.879	1.064
	0.141	0.137	1.047	0.921	1.478	0.770
Run 29	0.144	0.140	1.020	0.895	1.437	0.787
4/8	0.162	0.158	0.857	0.740	1.188	0.888
$A_p = 3.12 \times 10^{-3}$	0.187	0.183	0.717	0.606	0.973	1.029
	0.132	0.128	1.129	1.001	1.608	0.720
$\omega^* = 0.178$	0.134	0.130	1.092	0.967	1.550	0.730
	0.081	0.077	0.583	0.542	0.871	1.070
Run 30	0.069	0.065	0.790	0.743	1.194	0.903
4/8	0.061	0.057	0.910	0.862	1.387	0.792
$A_p = 3.12 \times 10^{-3}$	0.062	0.058	0.945	0.894	1.434	0.806
	0.058	0.054	1.029	0.974	1.569	0.751
$\omega^* = 0.072$	0.058	0.054	1.074	1.019	1.639	0.751

TABLE III (Cont.)

	ω_m	ω	$\theta \times 10^3$	$w \times 10^3$	A_∞/A_p	$\omega/\omega^*_{\not}$	ΔP_p	$\omega/\omega^*_{\neq}$
	0.073	0.069	0.477	0.447	0.718	1.328		
Run 30a	0.053	0.049	0.704	0.672	1.080	0.943		
4/8	0.047	0.043	0.897	0.860	1.381	0.828		
$A_p = 3.12 \times 10^{-3}$	0.045	0.041	0.991	0.952	1.530	0.790		
	0.044	0.040	1.047	1.005	1.613	0.770		
$\omega^* = 0.052$	0.043	0.039	1.070	1.040	1.670	0.750		
	0.044	0.040	1.089	1.043	1.680	0.770		
	0.040	0.040	1.103	1.061	1.710	0.770		
Run 31	0.047	0.043	0.851	0.818	0.981	1.000	+ 69	1.264
4/17	0.034	0.030	0.790	0.766	1.421	0.698	- 34	0.883
$A_p = 2.74 \times 10^{-3}$	0.031	0.027	0.964	0.938	1.740	0.628	-117	0.795
$\omega^*_{\not} = 0.043$	0.038	0.034	0.755	0.730	1.356	0.790	-1.0	1.000
$\omega^*_{\neq} = 0.034$								
Run 32								
4/20	0.034	0.031	0.823	0.798	1.464	0.722	- 23	0.939
$A_p = 2.74 \times 10^{-3}$	0.036	0.033	0.722	0.699	1.305	.769	+ 12	1.000
$\omega^*_{\not} = 0.043$	0.040	0.037	0.665	0.642	1.193	0.861	+ 30	1.120
$\omega^*_{\neq} = 0.033$	0.031	0.028	0.860	0.355	1.590	0.652	- 54	0.848

$\not$ Refers to ω^* obtained from area ratio calculation

$\neq$ Refers to ω^* from zero pressure differential

TABLE III (Cont.)

	ω_m	ω	$V \times 10^3$	$w \times 10^3$	A_∞ / A_p	$\omega/\omega^*_{\neq}$	ΔP_p	$\omega/\omega^*_{\neq}$
Run 33								
4/20	0.085	0.082	0.860	0.794	1.220	0.802	+ 39	1.109
$A_p = 2.74 \times 10^3$	0.081	0.078	0.875	0.813	1.250	0.763	+ 11	1.054
$\omega^*_{\neq} = 0.102$	0.076	0.073	0.974	0.906	1.393	0.714	- 23	0.987
$\omega^*_{\neq} = 0.074$	0.095	0.092	0.790	0.723	1.111	0.900	+ 66	1.243
Run 34								
$\omega^*_{\neq} = 0.043$	0.033	0.030	0.790	0.766	1.426	0.696	+ 17	1.070
$\omega^*_{\neq} = 0.028$	0.029	0.026	0.909	0.885	1.648	0.604	- 19	0.927
Run 35	0.034	0.031	0.714	0.690	1.282	0.815	+ 9	1.070
$\omega^*_{\neq} = 0.038$	0.029	0.026	0.860	0.839	1.560	0.684	- 28	0.897
$\omega^*_{\neq} = 0.028$	0.026	0.023	1.000	0.977	1.818	0.605	-110	0.794
Run 36	0.026	0.023	0.992	0.970	1.804	0.605	-140	0.742
$\omega^*_{\neq} = 0.038$	0.029	0.026	0.853	0.832	1.549	0.684	- 48	0.839
$\omega^*_{\neq} = 0.031$	0.035	0.032	0.681	0.660	1.228	0.833	+ 8	1.020
Run 37	0.050	0.047	0.669	0.639	1.188	0.813	- 2	0.980
$\omega^*_{\neq} = 0.057$	0.042	0.039	0.911	0.877	1.630	0.674	-105	0.813
$\omega^*_{\neq} = 0.048$	0.059	0.056	0.980	0.950	1.022	0.968	+ 27	1.169

$\neq$ Refers to ω^* obtained from area ratio calculation

$\neq$ Refers to ω^* obtained from zero pressure differential

APPENDIX D

Sample Calculations

From the measured inlet pressure and the curves of (1) the values of inlet Mach Number and injected water air ratio are found to be, for Run Number 23,

$$M_1 = 0.250$$

$$w_o = 0.038$$

These values are constant for the run.

From the calculations of Appendix B-3, the local Mach Number M_2 is calculated

$$\frac{M_2}{M_1} = \sqrt{\frac{-1+\sqrt{1+4(0.0130)(1.037)^2}}{2(0.0130)}} = 1.030$$

$$C_1 = (1.038)(0.2)(0.250)^2 = 0.0130$$

$$C_2 = \left[1+0.2(0.250)^2\right]\left(\frac{71.3}{70.5}\right)^2 = 1.037$$

$$M_2 = 1.030\,(0.250) = 0.2576$$

The local temperature T_2 is calculated from Equation (5) of Appendix B-3

$$T_2 = \frac{507}{1+(1.038)\,0.2\,(0.250)^2} = 500$$

The Area Ratio A_∞/A_p from Appendix B-4 is calculated to be

$$A_\infty/A_p = 5.64\,\frac{\sqrt{500}}{(70.5)(0.2576)}\,\frac{w_a}{2.74\times10^{-3}} = 2.536\times10^3\,w_a$$

The measured humidity and flow rate are calculated for the first point of Run 23, from Appendices B-1 and B-2,

DEW POINT 84.5 $P_{a_0} = 3.04 = (P_s)_+$

$P_d = 42.1$

$P_a = 39.06$

$\omega_m = 0.622\left(\frac{3.04}{39.06}\right) = 0.050$

$\omega = \omega_m - \omega_a = 0.044$

$$W = 0.579 \times 10^{-4}\sqrt{41.9\left(\frac{42.0}{13.6}\right)} = 0.660 \times 10^{-3}$$

The air mass flow rate through the probe and sampling system

$$\omega_a = \frac{W}{1+\omega} = \frac{0.660 \times 10^{-3}}{1.044} = 0.631 \times 10^{-3}$$

The value of A_ω/A_p is found from this value of ω_a to be

$$A_\omega/A_p = (2.536)(0.631) = 1.600$$

From ω vs. A_ω/A_p (Figure VI) the value of ω^* $\left[A_\omega/A_p = 1\right]$ is, $\omega^* = 0.062$

Hence

$$\omega/\omega^* = 0.710$$

APPENDIX I

TABLE IV

ORIGINAL DATA

	DEWCEL DATA			FLOW DATA	
	P_d	T_d	Dew Pt.	P_n	ΔP_n
	52.8	98	85	52.8	61.7
Run 14	41.7	84	77	47.4	98.5
3/25	29.0	76	66	29.8	157.0
II	24.4	76	61	25.7	189.0
T_o 510	23.8	76	60	25.1	193.1
ω_a 0.006	50.5	100	84	50.4	70.7
P_1 72.1	57.1	104	89	57.8	46.0
P_2 71.0	63.0	110	94	62.6	33.9
Rot. 30	70.9	110	106	70.7	11.8
	71.0	111	107	70.8	11.3
Run 15	74.5	120	113	73.3	33.2
3/27	57.2	122	106	57.1	51.4
II	49.5	116	99	49.6	74.8
T_o 506	58.4	118	108	58.2	48.8
ω_a 0.006	65.6	122	114	65.4	26.6
P_1 72.1	69.7	138	122	69.8	14.1
P_2 70.6	46.9	114	97	47.1	83.0
Rot. 60	43.3	103	95	43.6	94.8
Run 16	51.0	116	110	50.9	76.1
3/28	59.1	160	119	59.0	49.6
T_o 507	64.8	168	128	64.7	30.7
ω_a 0.005	47.5	134	108	48.5	86.4
P_1 66.4	39.8	122	101	40.1	113.3
P_2 64.1	35.3	114	97	35.7	137.5
Rot. 86	30.0	112	93	30.9	166.7

TABLE IV (Cont.)

	DEWCEL DATA			FLOW DATA	
	P_d	T_d	Dew Pt.	P_n	ΔP_n
Run 17	34.7	111	69	35.2	131.8
3/28	38.1	110	72	38.5	115.2
II	43.1	110	75	43.2	96.5
T_o 507	48.3	111	79	48.3	78.8
ω_a 0.005	55.9	111	84	55.8	55.2
P_1 66.4	62.2	111	91	62.1	36.5
	66.2	112	96	66.1	24.7
P_2 64.1	33.0	105	66	33.4	139.5
Rot. 30	69.9	114	103	69.9	13.2
Run 18					
3/28	67.2	138	118	67.1	21.6
II	61.9	139	110	61.8	38.5
T_o 507	62.1	139	111	61.8	38.5
ω_a 0.005	55.0	137	104	54.9	60.0
P_1 66.4	49.5	133	99	49.4	77.9
	35.0	124	88	35.4	134.6
P_2 64.1					
Rot. 60					
Run 19					
3/29	62.3	145	128	61.8	39.3
II	56.5	143	121	56.5	57.5
T_o 503	49.4	139	114	49.4	80.5
ω_a 0.005	42.4	134	106	43.1	107.5
P_1 66.5	35.9	130	100	36.5	135.1
	31.7	125	96	32.5	160.2
P_2 62.7	29.3	122	95	30.0	177.5
Rot. 90					

TABLE IV (Cont.)

	DEWCEL DATA			FLOW DATA	
	P_d	T_d	Dew Pt.	P_n	ΔP_n
Run 20	60.7	133	111	60.3	39.0
3/29	60.8	123	113	60.7	38.7
II	55.7	133	108	55.6	54.0
T_o 503	55.9	133	107	55.7	55.0
ω_a 0.005	49.4	130	100	49.2	74.0
P_1 61.7	43.8	128	96	43.9	93.1
P_2 56.3	37.9	126	92	38.0	116.3
Rot. 60					
Run 22	41.5	132	80	41.6	94.5
3/29	46.7	132	84	46.7	75.0
IV	51.1	132	87	51.1	64.5
T_o 503	57.2	132	93	57.0	48.0
ω_a 0.005	61.3	133	97	61.1	36.0
P_1 72.7	66.3	133	103	66.2	23.0
P_2 71.4					
Rot. 62					
Run 23	42.1	99	85	41.9	42.0
3/30	35.0	99	78	34.8	55.0
III	27.1	97	70	26.9	73.3
T_o 507	21.0	89	62	21.0	93.7
ω_a 0.006	18.5	86	58	18.6	106.2
P_1 71.3	48.0	109	90	47.9	32.1
P_2 70.5	54.7	120	95	54.5	23.3
Rot. 30	59.9	123	103	58.7	16.6

TABLE IV (Cont.)

	DENCEL DATA			FLOW DATA	
	P_d	T_d	Dew Pt.	P_n	ΔP_n
Run 24					
3/30	61.5	140	123	59.3	16.1
III	45.3	140	102	45.1	38.7
T_o 503	38.1	133	94	34.9	57.7
ω_a 0.006	22.6	112	79	22.4	93.0
P_1 71.3	18.5	116	73	18.6	112.0
P_2 70.5	55.8	132	112	55.7	23.2
Rot. 60					
Run 25					
3/30					
III	58.0	141	129	58.0	20.5
T_o 503	49.1	141	116	49.0	34.2
ω_a 0.006	48.9	137	116	48.9	34.1
P_1 71.3	39.9	133	107	39.5	50.0
P_2 70.5	29.8	126	97	29.6	72.0
Rot. 90					
Run 27					
4/7					
IIA	42.8	140	101	43.0	95.5
T_o 507	47.2	140	105	47.2	78.0
ω_a 0.006	54.1	143	113	54.0	52.5
P_1 63.0	60.8	145	123	60.7	29.6
P_2 58.2	65.7	146	133	65.6	14.9
Rot. 66					

TABLE IV (Cont.)

	DEWCEL DATA			FLOW DATA	
	P_d	T_d	Dew Pt.	P_n	ΔP_n
Run 28					
4/7	30.8	164	93	31.7	170.1
IIA	33.7	164	96	34.5	152.5
T_o 511	37.3	165	98	37.8	133.8
ω_a 0.006	42.7	165	103	43.0	106.0
P_1 69.7	48.2	166	108	48.3	83.7
P_2 67.3	58.6	166	120	58.5	45.7
Rot. 76	64.5	128	10.62	64.5	25.8
Run 29					
4/8	39.5	138	114	38.6	119.6
IIA	45.3	140	119	46.1	92.2
T_o 511	55.4	149	130	55.8	53.6
ω_a 0.004	61.6	152	138	61.6	34.0
P_1 69.7	35.5	148	108	37.4	138.6
P_2 67.3	38.4	149	111	39.6	124.0
Rot. 114					
Run 30					
IIA	65.7	150	11[illegible]	[illegible]	21.0
T_o 511	57.6	147	104	57.6	44.0
ω_a 0.004	50.8	144	98	51.3	65.5
P_1 69.7	48.2	142	96	48.7	74.2
P_2 67.3	40.9	138	89	41.8	103.0
Rot. 51	34.8	130	84	36.0	132.6

TABLE IV (Cont.)

	DEWCEL DATA			FLOW DATA		
	P_d	T_d	Dew Pt.	P_n	ΔP_n	ΔP_p
Run 30_a 4/7 IIA	29.0	135	71	30.7	163.8	
	31.8	135	74	33.3	147.0	
	35.0	135	76	36.2	129.5	
T_o 511	38.1	136	79	39.2	113.9	
ω_a 0.004	43.6	136	84	44.3	90.3	
P_1 69.7	51.3	137	90	51.7	63.0	
P_2 67.3	61.5	139	100	61.5	32.8	
Rot. 51	68.4	140	113	68.4	13.5	
Run 31 4/17 IV	67.6	123	99	67.5	18.3	+69
T_o 511	56.7	121	84	56.6	50.3	-34
ω_a 0.004	45.6	120	74	45.6	83.5	-117
P_1 69.0	61.1	122	89	60.8	38.5	- 1
P_2 67.4						
Rot 36						
Run 32 4/20 IV	57.5	115	84	57.5	48.0	-23
T_o 505	62.0	115	88	61.8	34.6	+12
ω_a 0.003	64.0	115	92	63.8	28.5	+30
P_1 68.7	53.6	113	79	53.6	59.2	-54
P_2 67.2						
Rot 36						

TABLE IV (Cont.)

		DEWCEL DATA			FLOW DATA		
		P_d	T_d	Dew Pt.	P_n	ΔP_n	ΔP_p
Run 33 4/20 IV							
T_o	505	55.5	127	111	55.4	53.9	+39
ω_a	0.003	51.9	128	107	52.0	65.3	+11
P_1	65.7	47.0	127	102	47.1	80.6	-23
P_2	61.8	59.3	128	116	59.1	42.6	+66
Rot	92						
		59.4	124	84	59.2	42.6	+17
Runs 34-37 4/20		51.8	121	75	51.8	65.0	-19
		62.4	122	87	62.2	33.1	+ 9
T_o	505	55.3	121	79	55.3	53.8	-28
ω_a	0.003	42.5	112	67	42.8	93.6	-117
P_1	68.7	42.8	109	68	42.8	93.2	-140
		55.3	110	79	55.0	53.7	-48
P_2	67.2	64.1	111	88	62.9	30.3	+ 8
Rot.	36	62.2	112	97	62.0	29.5	- 2
		49.4	111	85	49.4	66.0	-105
		65.1	122	105	65.0	21.0	+27

APPENDIX F

Literature Citations

1. Kesler, G. H., "Mass Transport in Spray-Laden Air Streams", MIT ScD Thesis, 1952.

2. Langmuir, I., and Blodgett, K., "A Mathematical Investigation of Water Drop Trajectories", Technical Report 5418, Air Material Command, AAF, February 19, 1946.

3. Neel, C. B., Jr., and Steinmetz, C. P., "The Calculated and Measured Performance Characteristics of a Heated-Wire-Water-Content Meter for Measuring Icing Severity", NACA TN 2615, January 1952.

4. Wadliegh, K. R., "An Experimental Investigation of a Small Scale Aerothermopressor - A Device for Increasing the Stagnation Pressure of a High Velocity, High Temperature Gas Stream by Evaporative Cooling", MIT ScD Thesis, June 1953.

5. Larson, H. K., "A Technique for Measuring Specific Humidity of the Gas Phase of a High Temperature, High Velocity, Two Phase Stream of Air and Water", MIT M.S. Thesis, in preparation.

6. ASME "Power Test Codes, Part 5, Chapter 4 - Flow Measurement by Means of Standardized Nozzles and Orifice Plates", Table 7, pp 30.

7. Shapiro, A. H., Hawthorne, W. R., and Edelman, G. M., "The Mechanics and Thermodynamics of Steady One-Dimensional Gas Flow", Meteor Report No. 14, December 1947.

8. Lewis, W., and Jones, A. R., "A Review of Instruments Developed for the Measurement of the Meteorlogical Factors Conducive to Aircraft Icing", NACA RM A9C09, April 1949.

9. Shapiro, A. H. and Smith, R. D., "Friction Coefficients in the Inlet Length of Smooth Round Tubes", NACA TN 1785, November 1948.

10. Bemis, J. R. and Houghton, H. G., "Instruments for the Determination of Rain Densities in Flight", NACA ARR3E18 (WR W-42) May 1943.

11. Perkins, P. J., "Flight Instruments for Measurement of Liquid-water Content in Clouds at Temperatures Above or Below Freezing", NACA RME50J12A, March 1951.

12. Tolefson, H. B., "Flight Measurement of Liquid-Water Content of Clouds and Precipitation Regions", NACA RB L4E17, May 1944.

13. Malkus, W.V.R., Bishop, R. H., and Briggs, R. O., "Analysis and Preliminary Design of an Optical Instrument for Measurement of Drop Size and Free Water Content of Clouds", NACA TN1622, June 1948.

14. Gisvold, P. A. and Matheson, J. C., "Small Scale Constant-Area Test of an Aerothermopressor", MIT Nav. Eng. Thesis, 1952.

JUL 2 BINDERY

Thesis
K827 Kosiba
20526
A sampling technique for the measurement of the water air ratio of a high speed spray laden air stream.
BINDERY

Thesis
K827 Kosiba
20526
A sampling technique for the measurement of the water air ratio of a high speed spray laden air stream.

Library
U. S. Naval Postgraduate School
Monterey, California

ARTISAN GOLD LETTERING AND SMITH BINDERY OAKLAND, CALIF.

thesK827
A sampling technique for the measurement
3 2768 002 10500 9
DUDLEY KNOX LIBRARY